Article
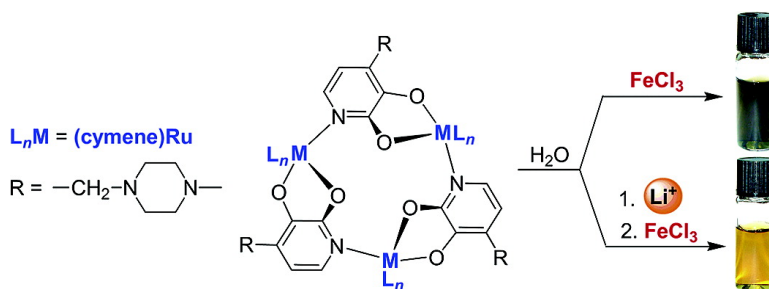
pH-Triggered Assembly of Organometallic Receptors for Lithium Ions

Zacharias Grote, Rosario Scopelliti, and Kay Severin

More About This Article

Additional resources and features associated with this article are available within the HTML version:

- Supporting Information
- Links to the 8 articles that cite this article, as of the time of this article download
- Access to high resolution figures
- Links to articles and content related to this article
- Copyright permission to reproduce figures and/or text from this article

View the Full Text HTML

pH-Triggered Assembly of Organometallic Receptors for Lithium Ions

Zacharias Grote, Rosario Scopelliti, and Kay Severin*

*Contribution from the Institute of Chemical Sciences and Engineering,
Swiss Federal Institute of Technology Lausanne (EPFL), 1015 Lausanne, Switzerland*

Received August 25, 2004; E-mail: kay.severin@epfl.ch

Abstract: The reaction of half-sandwich complexes of ruthenium, rhodium, and iridium with amino-substituted 3-hydroxy-2-pyridone ligands in aqueous solution gives monomeric O,O'-chelate complexes. Upon addition of base, the complexes assemble to form trimeric metallamacrocycles, as evidenced by NMR spectroscopy and single-crystal X-ray analyses. The macrocycles are able to act as highly selective receptors for lithium ions. The binding constants depend on the nature of the half-sandwich complex, the ligand, and the pH. With a commercially available (cymene)Ru complex, a receptor with a Li^+ binding constant of $K_a = 5.8$ $(\pm 1.0) \times 10^4 \ M^{-1}$ and a $Li^+–Na^+$ selectivity of 10 000:1 can be obtained. The fact that the assembly process of the receptor is pH-dependent can be used to detect the presence of lithium ions by a pH measurement. Furthermore, it is possible to transduce the binding of Li^+ into a change of color by means of a chemical reaction with $FeCl_3$. This allows the detection of Li^+ in the pharmacologically relevant concentration range of 0.5–1.5 mM by the "naked eye".

Introduction

In 1949, John Cade reported that lithium salts have a calming effect on patients with acute mania.[1] The potential value in psychiatry was subsequently confirmed by many other studies, and since the mid-1960s, lithium salts are among the most frequently used drugs for patients suffering from bipolar disorder.[2] Recent studies suggest that lithium could also be used for the treatment of Alzheimer's disease[3] and of schizophrenia, and it was speculated whether lithium could become the "aspirin of the brain".[4] Apart from applications in the field of psychiatry and neurology, lithium salts have been employed to treat skin diseases, were shown to inhibit the replication of certain viruses, and can affect the immune response.[2b]

Given the pharmacological relevance, it is not surprising that considerable efforts have been devoted toward the development of sensors for lithium ions.[5] From a chemical point of view, the synthesis of specific receptors is of special interest. So far, most investigations have focused on organic macrocycles, which are generally employed in a nonaqueous environment.[5,6] The design of synthetic receptors, which can be used directly in water, represents a special challenge. First, the host needs to be soluble in water. This severely limits the type of building blocks which can be employed to construct the receptor. Second,

the hydration energy of Li^+ is very high (519 kJ mol^{-1}).[7] As a consequence, the binding constants of artificial hosts are significantly lower in water when compared to those in organic solvents. The Li^+-specific ionophore, 12-crown-4, for example, displays a binding constant of log $K = 4.25$ in acetonitrile, whereas in water, no interaction with Li^+ could be detected at all (log $K \approx 0$).[8] Among the few receptors which are able to bind Li^+ in water with high affinity, azamacrobicyclic cage molecules play a dominant role.[9,10] One of the highest stability constants was found for the cryptand (2,1,1) (log $K = 5.5$).[9g] This receptor also displays a good selectivity for Li^+ over Na^+ (200:1). For potential applications, however, azamacrobicyclic receptors show a severe disadvantage; the synthesis of these compounds generally requires several steps and proceeds with modest overall yields.[9]

In the continuation of our studies of metallamacrocyclic hosts,[11,12] we have recently described a potent and selective

(1) Cade, J. F. J. *Med. J. Aust.* **1949**, *2*, 349–352.
(2) (a) McIntyre, R. S.; Mancini, D. A.; Parikh, S.; Kennedy, S. H. *Can. J. Psychiatry* **2001**, *46*, 322–327. (b) Birch, N. J. *Chem. Rev.* **1999**, *99*, 2659–2682. (c) Dalay, I. *Lancet* **1997**, *349*, 1157–1160.
(3) (a) Phiel, C. J.; Wilson, C. A.; Lee, V. M.-Y.; Klein, P. S. *Nature* **2003**, *423*, 435–439. (b) De Strooper, B.; Woodgett, J. *Nature* **2003**, *423*, 392–393.
(4) Pilcher, H. R. *Nature* **2003**, *425*, 118–120.
(5) (a) Bartsch, R. A.; Ramesh, V.; Bach, R. O.; Shono, T.; Kimura, K. In *Lithium Chemistry*; Sapse, A.-M., von Ragué Schleyer, P., Eds.; John Wiley & Sons: New York, 1995; pp 393–476. (b) Christian, G. D. *Sensors* **2002**, *2*, 432–435. (c) Christian, G. D. *J. Pharm. Biomed. Anal.* **1996**, *14*, 899–908.

(6) For some selected recent publications, see: (a) Gunnlaugsson, T.; Bichell, B.; Nolan, C. *Tetrahedron* **2004**, *60*, 5799–5806. (b) Tsuchiya, S.; Nakatani, Y.; Ibrahim, R.; Ogawa, S. *J. Am. Chem. Soc.* **2002**, *124*, 4936–4937. (c) Gunnlaugsson, T.; Bichell, B.; Nolan, C. *Tetrahedron Lett.* **2002**, *43*, 4989–4992. (d) Qin, W.; Obare, S. O.; Murphy, C. J.; Angel, S. M. *Anal. Chem.* **2002**, *74*, 4757–4762. (e) Talanova, G. G.; Talanov, V. S.; Hwang, H.-S.; Eliasi, B. A.; Bartsch, R. A. *J. Chem. Soc., Perkin Trans. 2* **2002**, 1869–1874. (f) Obare, S. O.; Murphy, C. J. *Inorg. Chem.* **2001**, *40*, 6080–6082. (g) Paquette, L. A.; Tae, J. *J. Am. Chem. Soc.* **2001**, *123*, 4974–4984. (h) Chen, J.-A.; Lai, J.-L.; Lee, G. H.; Wang, Y.; Su, J. K.; Yeh, H.-C.; Lin, W.-Y.; Leung, M.-K. *Org. Lett.* **2001**, *3*, 3999–4002. (i) Chen, Y.; Yang, F.; Gong, S. *Tetrahedron Lett.* **2000**, *41*, 4815–4818. (j) Paquette, L. A.; Tae, J.; Hickey, E. R.; Rogers, R. D. *Angew. Chem., Int. Ed.* **1999**, *38*, 1409–1411. (k) Inokuma, S.; Takezawa, M.; Satoh, H.; Nakamura, Y.; Sasaki, T.; Nishimura, J. *J. Org. Chem.* **1998**, *63*, 5791–5796. (l) Tsukube, H.; Shinoda, S.; Mizutani, Y.; Okano, M.; Takagi, K.; Hori, K. *Tetrahedron* **1997**, *53*, 3487–3496. (m) Bockstahl, F.; Graf, E.; Hosseini, M. W.; Suhr, D.; De Cian, A.; Fischer, J. *Tetrahedron Lett.* **1997**, *38*, 7539–7542. (n) Kobiro, K. *Coord. Chem. Rev.* **1996**, *148*, 135–149. (o) Faulkner, S.; Kataky, R.; Parker, D.; Teasdale, A. *J. Chem. Soc., Perkin Trans. 2* **1995**, 1761–1769.
(7) Cotton, F. A.; Wilkinson, G.; Murillo, C. A.; Bochmann, M. *Advanced Inorganic Chemistry*, 6th ed.; John Wiley & Sons: New York, 1999; p 102.
(8) Smetana, A. J.; Popov, A. I. *J. Solution Chem.* **1980**, *9*, 183–186.

Scheme 1
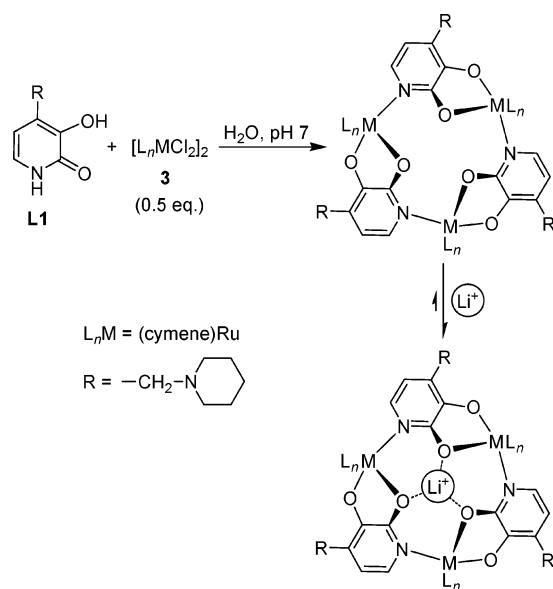
receptor for Li$^+$ in water (log K = 3.4).[13] The synthesis of this receptor is remarkably simple; it forms in nearly quantitative yield if the hydroxypyridone ligand **L1** is dissolved together with the (arene)Ru complex **3** in water containing phosphate buffer (Scheme 1). In the following, it will be shown that it is possible to increase the Li$^+$ affinity for this type of receptor by more than 1 order of magnitude using simple structural modifications. Furthermore, it will be demonstrated that the self-assembly process of the metallamacrocycle is strongly pH-dependent. This provides the opportunity to detect lithium ions by a simple pH measurement. In addition, a colorimetric test will be described, which allows one to sense lithium ions in water at the pharmacologically relevant concentration range of 0.5−1.5 mM.[5]

Results and Discussion

pH-Triggered Assembly. Ligands **L1**−**L4** were chosen for the synthesis of water-soluble receptors because (a) they contain
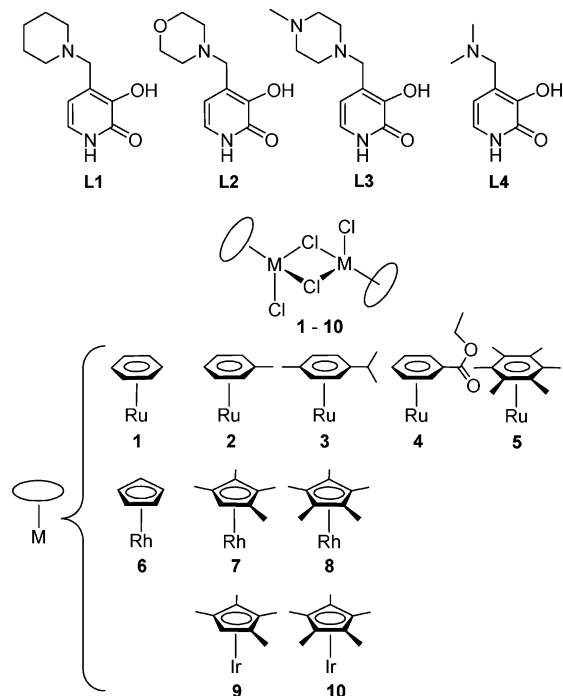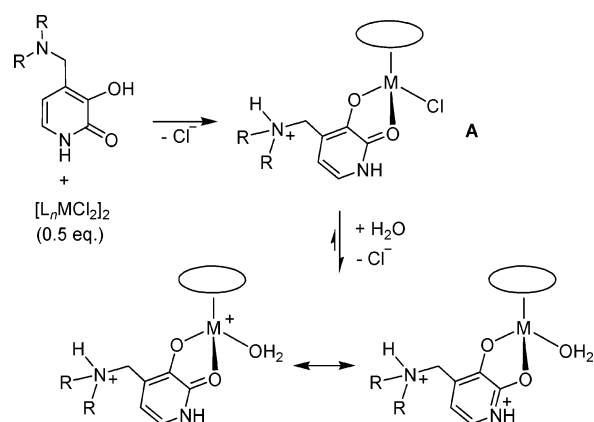
(9) (a) Dapporto, P.; Formica, M.; Fusi, V.; Giorgi, L.; Micheloni, M.; Pontellini, R.; Paoli, P.; Rossi, P. *Eur. J. Inorg. Chem.* **2001**, 1763−1774. (b) Micheloni, M.; Formica, M.; Fusi, V.; Romani, P.; Pontellini, R.; Dapporto, P.; Paoli, P.; Rossi, P.; Valtancoli, B. *Eur. J. Inorg. Chem.* **2000**, 51−57. (c) Bencini, A.; Fusi, V.; Giorgi, C.; Micheloni, M.; Nardi, N.; Valtancoli, B. *J. Chem. Soc., Perkin Trans. 2* **1996**, 2297−2302. (d) Bencini, A.; Bianchi, A.; Chimichi, S.; Ciampolini, M.; Dapporto, P.; Garcia-España, E.; Micheloni, M.; Nardi, N.; Paoli, P.; Valtancoli, B. *Inorg. Chem.* **1991**, *30*, 3687−3691. (e) Bencini, A.; Bianchi, A.; Borselli, A.; Chimichi, S.; Ciampolini, M.; Dapporto, P.; Micheloni, M.; Nardi, N.; Paoli, P.; Valtancoli, B. *Inorg. Chem.* **1990**, *29*, 3282−3286. (f) Bencini, A.; Bianchi, A.; Borselli, A.; Ciampolini, M.; Garcia-España, E.; Dapporto, P.; Micheloni, M.; Paoli, P.; Ramirez, J. A.; Valtancoli, B. *Inorg. Chem.* **1989**, *28*, 4279−4284. (g) Cox, B. G.; Garcia-Rosas, J.; Schneider, H. *J. Am. Chem. Soc.* **1981**, *103*, 1384−1389.

(10) For an innovative alternative approach, which is based on sensing with gold nanoparticles, see: Obare, S. O.; Hollowell, R. E.; Murphy, C. J. *Langmuir* **2002**, *18*, 10407−10410.

(11) (a) Lehaire, M.-L.; Scopelliti, R.; Herdeis, L.; Polborn, K.; Mayer, P.; Severin, K. *Inorg. Chem.* **2004**, *43*, 1609−1617. (b) Lehaire, M.-L.; Schulz, A.; Scopelliti, R.; Severin, K. *Inorg. Chem.* **2003**, *42*, 3576−3581. (c) Lehaire, M.-L.; Scopelliti, R.; Severin, K. *Angew. Chem., Int. Ed.* **2002**, *41*, 1419−1421. (d) Lehaire, M.-L.; Scopelliti, R.; Severin, K. *Chem. Commun.* **2002**, 2766−2767. (e) Lehaire, M.-L.; Scopelliti, R.; Severin, K. *Inorg. Chem.* **2002**, *41*, 5466−5474. (f) Piotrowski, H.; Severin, K. *Proc. Natl. Acad. Sci. U.S.A.* **2002**, *99*, 4997−5000. (g) Piotrowski, H.; Hilt, G.; Schulz, A.; Mayer, P.; Polborn, K.; Severin, K. *Chem.—Eur. J.* **2001**, *7*, 3196−3208. (h) Piotrowski, H.; Polborn, K.; Hilt, G.; Severin, K. *J. Am. Chem. Soc.* **2001**, *123*, 2699−2700.

(12) Severin, K. *Coord. Chem. Rev.* **2003**, *245*, 3−10.

(13) Grote, Z.; Lehaire, M.-L.; Scopelliti, R.; Severin, K. *J. Am. Chem. Soc.* **2003**, *125*, 13638−13639.

Figure 1. Ligands (**L1**−**L4**) and half-sandwich complexes (**1**−**10**), which were employed to generate metallamacrocycles.
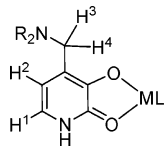
the 3-hydroxy-2-pyridone structural motif, which favors the formation of trinuclear metallamacrocycles,[11] and (b) they contain a tertiary amino group, which is able to enhance the solubility of the resulting complexes without interfering with the self-assembly process (Figure 1). All ligands can be prepared in a Mannich reaction of 3-hydroxy-2-pyridone, formaldehyde, and the corresponding amine.[14] For the reaction partner, we have employed organometallic half-sandwich complexes of ruthenium (**1**−**5**), rhodium (**6**−**8**), and iridium (**9** and **10**). These complexes are either commercially available (**1**, **3**, **8**, and **10**) or easily accessible.

First, we investigated the reaction of complexes **1**−**10** with ligands **L1**−**L4** in plain water. When the chloro-bridged half-sandwich complexes were stirred with 2 equiv of the respective ligand, clear yellow to orange solutions were obtained after several minutes. ^{1}H NMR spectroscopic investigation of the resulting mixtures showed the presence of a single complex. Given the known tendency of hydroxypyridone ligands to form O,O'-chelates with half-sandwich complexes,[11g,15] it appeared

Scheme 2

Table 1. Selected ^{1}H NMR Signals (ppm) of Monomeric Half-Sandwich Complexes Obtained by Reaction of Complexes **1**–**10** with Ligands **L1**–**L4** in D_2O

entry	complex	ligand	H$^{1\,a}$	H$^{2\,a}$	H$^{3/4}$
1		**L1**	6.69	6.28	4.05
2		**L2**	7.02	6.38	3.73
3		**L3**	6.90	6.33	3.70
4		**L4**	6.62	6.20	3.98
5	**1**	**L1**	6.91	6.53	4.22
6	**1**	**L3**	6.91	6.55	3.68
7	**2**	**L1**	6.92	6.53	4.23
8	**2**	**L3**	6.89	6.54	3.71
9	**3**	**L1**	6.88	6.49	4.21
10	**3**	**L2**	6.90	6.53	4.33
11	**3**	**L3**	6.88	6.53	3.70
12	**3**	**L4**	6.70	6.50	4.25
13	**4**	**L1**	6.92	6.70	4.23
14	**4**	**L3**	6.91	6.55	3.75
15	**5**	**L1**	6.82	6.46	4.21
16	**5**	**L2**	6.81	6.46	4.27
17	**5**	**L3**	6.81	6.49	3.69
18	**5**	**L4**	6.82	6.46	4.27
19	**6**	**L1**	6.92	6.53	4.19
20	**6**	**L3**	6.92	6.57	3.70
21	**7**	**L1**	6.74	6.38	4.09
22	**7**	**L3**	6.84	6.51	3.74
23	**8**	**L1**	6.81	6.45	4.18
24	**8**	**L3**	6.82	6.49	3.72
25	**9**	**L1**	6.89	6.50	4.21
26	**9**	**L3**	6.89	6.52	3.78
27	**10**	**L1**	6.89	6.49	4.23
28	**10**	**L3**	6.86	6.50	3.77

^{a} The signals appear as doublets with a coupling constant of $^3J_{H-H} = 7$ Hz.

likely that mononuclear complexes of type A had formed (Scheme 2). This was confirmed for three examples by single-crystal X-ray analysis (see below).

The chloro ligands of type A complexes are expected to be labile because upon abstraction of the ligand, a cationic complex is formed, which can be described by two mesomeric forms: one in which the positive charge is located at the metal and another in which the positive charge is localized on the ring nitrogen atom (Scheme 2). In a good donor solvent, such as water, it is thus expected that the chloro ligands are substituted. The following experiments suggest that this is indeed the case. An aqueous solution (D_2O) containing the monomeric complex formed from **3** and **L1** was treated with 10 equiv of $AgNO_3$. A white precipitate of AgCl formed immediately, which was separated by filtration. The ^{1}H NMR spectrum of the resulting complex was identical to that of the starting material, indicating that the nature of the anion (NO_3^- vs Cl^-) has a minor effect on the ruthenium complex. Similar results were obtained with the rhodium and iridium complexes obtained from **L1** and **8** or **10**, respectively.

The coordination of the metal to the oxygen atoms of the ligand results in a translocation of a proton from the hydroxy to the amine group. This is reflected by the chemical shift of the signals for the methylene group next to the nitrogen atom (H$^{3/4}$, Table 1). While for the free ligands, the signals of these protons appear between $\delta = 3.70$ and 4.05 ppm (Table 1, entries
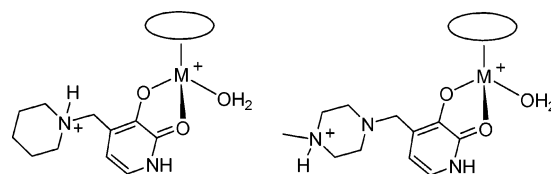
Figure 2. Monomeric half-sandwich complexes containing ligands **L1** (left) and **L3** (right).
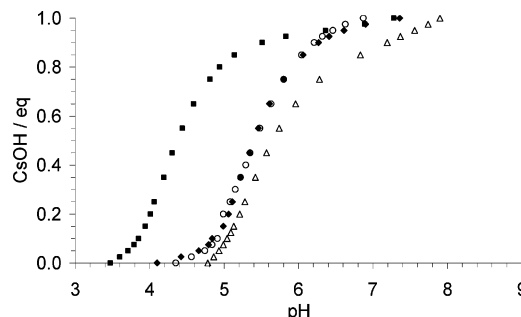
Figure 3. The pH of solutions containing ligand **L1** (15.0 mM) and complexes **1** ($\triangle$), **2** ($\bigcirc$), **3** ($\blacklozenge$), and **4** ($\blacksquare$) (Ru concn = 15.0 mM) after addition of increasing amounts of CsOH (0–1.0 equiv).

1–4), the corresponding signals for the metal complexes with **L1**, **L2**, and **L4** appear between $\delta = 4.09$ and 4.33 ppm, in agreement with the presence of a protonated amine group. For complexes with ligand **L3**, on the other hand, the signals of the methylene protons are only slightly shifted. This indicates that it is predominantly the terminal nitrogen atom of the piperazine group, which is protonated (Figure 2). The fact that the MeNR$_2$ nitrogen of ligand **L3** is more basic was confirmed in NMR titration experiments with DCl. Upon addition of incremental amounts of DCl (0–2.0 equiv) to a solution of ligand **L3**, it was first the signals of the protons close to the MeNR$_2$ group which were shifted. Significant differences in chemical shifts for the H$^{3/4}$ protons (Table 1) were only observed upon addition of more than 1.0 equiv of DCl.

Next, the influence of the pH was investigated using potentiometric titrations. Increasing amounts of CsOH (0–1.0 equiv) were added to solutions of type A monomeric complexes (15.0 mM). In all cases, a pH profile characteristic of a weak acid was obtained. The data obtained for ruthenium complexes **1**–**4** and ligand **L1** are depicted in Figure 3;[16] the corresponding data for rhodium and iridium complexes **6**–**10** are shown in Figure 4.

Ruthenium complexes **1**–**3** all behave very similar, with an inflection point at a pH of ~5.5. The ($C_6H_5CO_2Et$)Ru complex, **4**, having an electron-withdrawing ester side chain, on the other hand, is slightly more acidic, with an inflection point at pH 4.3. The acidity of the complexes is not only affected by the nature of the π-ligand but also by the metal ion. This is evidenced by comparing the data of rhodium complexes **7** and **8** with those of iridium complexes **9** and **10** (Figure 4). Clearly, the iridium complexes are more acidic than the rhodium complexes having the same type of ligands (**7** vs **9** and **8** vs **10**).

(14) (a) Nakamura, A.; Shozo, K. *Chem. Pharm. Bull.* **1968**, *16*, 1466–1471. (b) Osborne, A. G.; Jackson, L. *Spectrochim. Acta* **1993**, *49A*, 1703–1708. (c) Patel, M. K.; Fox, R.; Taylor, P. D. *Tetrahedron* **1996**, *52*, 1835–1840. (d) Chi, K.-W.; Ahn, Y. S.; Park, T. H.; Ahn, J. S.; Kim, H. A.; Park, J. Y. *J. Korean Chem. Soc.* **2001**, *45*, 51–60.

(15) (a) Lang, R.; Polborn, K.; Severin, T.; Severin, K. *Inorg. Chim. Acta* **1999**, *294*, 62–67. (b) Carter, L.; Davies, D. L.; Fawcett, J.; Russel, D. R. *Polyhedron* **1993**, *12*, 1599–1602.

(16) The hexamethylbenzene complex **5** was not included in this study because of the low solubility of the resulting complexes in water.
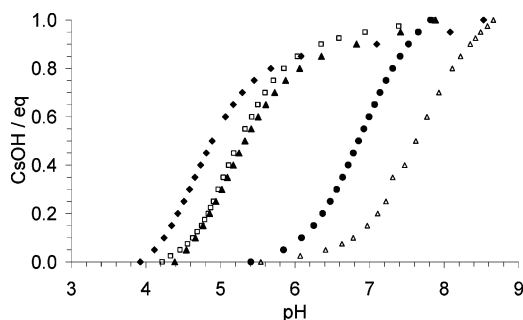
Figure 4. The pH of solutions containing ligand **L1** (15.0 mM) and complexes **6** (▲), **7** (●), **8** (△), **9** (◆), and **10** (□) (Rh/Ir concn = 15.0 mM) after addition of increasing amounts of CsOH (0−1.0 equiv).

When combined with (cymene)Ru complex **3**, pyridone ligands **L1**, **L2**, and **L4** gave rise to very similar pH profiles with pK_a = 5.4. For the piperazine ligand **L3**, on the other hand, the inflection point was found at slightly higher pH (pK_a = 6.9).

For some metal−ligand combinations, precipitation occurred after addition of 1.5−2 equiv of CsOH (pH ≈ 9.0−10.5, metal concn = 15 mM). This indicates that the fully deprotonated complexes display a lower solubility in water. There are various metal−ligand mixtures, however, for which no precipitation was observed after addition of 2 equiv of CsOH. In particular, complexes with (C_6H_6)Ru− (**1**), (C_6H_5Me)Ru− (**2**), and CpRh (**6**) show a relatively high solubility (≥5 mM), even in the fully deprotonated form. The solubility was not only influenced by the metal fragment but also by the ligand. In general, the solubility increased in the following order: **L1** < **L2** ∼ **L4** < **L3**.

To obtain more information about the complexes which are formed at different pH values, we have performed NMR titration experiments for selected metal−ligand combinations. Part of the ^{1}H NMR spectra obtained for a mixture of (cymene)Ru complex **3** and ligand **L1** upon addition of CsOH (0−1.0 equiv) is shown in Figure 5. For the monomeric complex obtained in plain D_2O (spectrum e), one can observe a singlet for the NCH_2 group at 4.21 ppm, two doublets between 5.5 and 6.0 ppm for the aromatic CH protons of the cymene π-ligand, and two doublets between 6.5 and 7.0 ppm for pyridone CH protons. Upon addition of CsOH, we can detect the signals of a second complex. The latter is completely dominating the solution after addition of 1 equiv of CsOH. The signals of the new complex
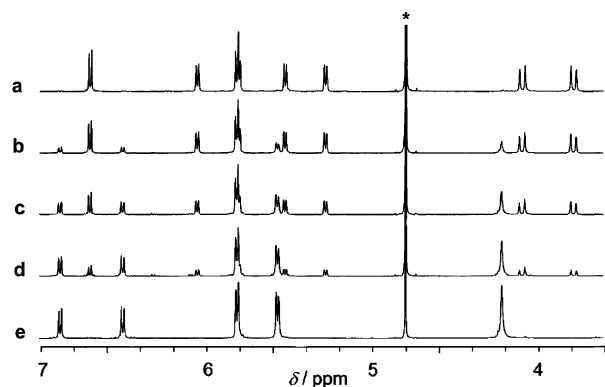

Figure 5. Part of the ^{1}H NMR spectrum (D_2O) of a solution containing [(cymene)RuCl$_2$]$_2$ (**3**) (7.5 mM) and ligand **L1** (15.0 mM) after addition of different amounts of CsOH: (a) 1.00, (b) 0.75, (c) 0.50, (d) 0.25, and (e) 0.00 equiv. Spectrum "a" corresponds to trimer B, and spectrum "e" corresponds to monomer A. The solvent peak is denoted by an asterisk (∗).

Figure 6. Part of the ^{1}H NMR spectrum (D_2O) of a solution containing [(C_5Me_4H)IrCl$_2$]$_2$ (**9**) (7.5 mM) and ligand **L1** (15.0 mM) after addition of different amounts of CsOH: (a) 1.00, (b) 0.75, (c) 0.50, (d) 0.25, and (e) 0.00 equiv. Spectrum "a" corresponds to trimer B, and spectrum "e" corresponds to monomer A. The solvent peak is denoted by an asterisk (∗).
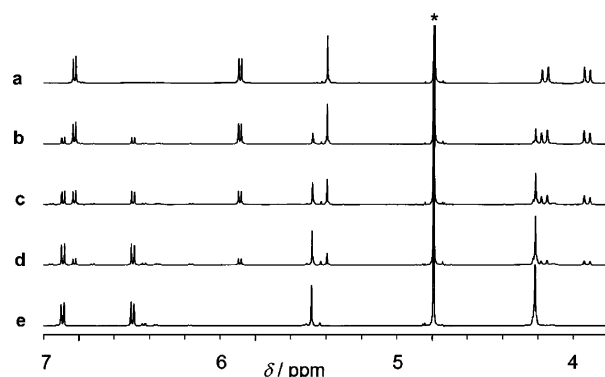
are very similar to those found for mixtures of **3** and **L1** in phosphate buffer (pH 7.0)[13] and can be assigned to a trimeric macrocycle of type B (Scheme 3). An important difference

Scheme 3
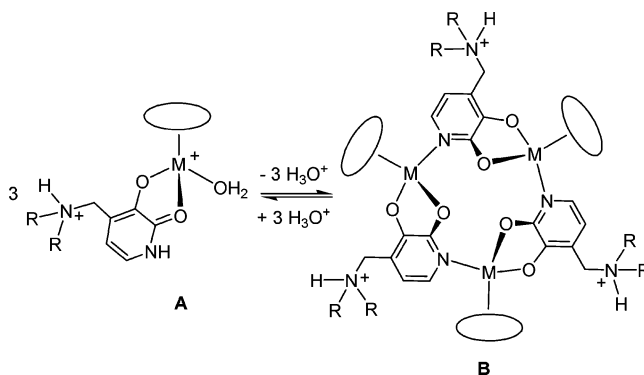
between the spectra of the monomeric and the trimeric complex is the multiplicity of the aromatic CH protons of the cymene π-ligand and of the NCH_2 protons. Although the metals represent stereogenic centers in both complexes, only the rigid metallamacrocycle is conformationally stable on the NMR time scale. As a consequence, we can observe two doublets for the diastereotopic NCH_2 protons at ∼4 ppm and four doublets for the cymene CH protons between 5.2 and 6.2 ppm (Figure 5a).

NMR titration experiments using iridium complex **9** and ligand **L1** gave similar results; upon addition of CsOH, one could observe the signals of a second complex (Figure 6). With 1 equiv of CsOH, this complex is the dominant species in solution (>95%). The two doublets for the NCH_2 protons confirm the presence of a chiral complex, which is conformationally stable on the NMR time scale.

The ^{1}H NMR data described above are in agreement with a pH-dependent self-assembly process, as shown in Scheme 3.[17] After deprotonation of the pyridone, the ring nitrogen is able to coordinate to a metal, thereby replacing a weakly bound water ligand. The pH at wich 50% of monomer A is converted to trimer B varies substantially (Figures 3 and 4). It is plausible that steric effects influence the aggregation, but electronic effects

(17) The pH-dependent assembly of Cp*Rh complexes using nucleobase ligands has been investigated extensively by Fish's group: (a) Fish, R. H.; Jaouen, G. *Organometallics* **2003**, *22*, 2166−2177. (b) Fish, R. H. *Coord. Chem. Rev.* **1999**, *185−186*, 569−584.

Figure 7. Part of the ^1H NMR spectrum (D_2O) of a solution containing $[(C_5Me_4H)RhCl_2]_2$ (7.5 mM) and ligand **L1** (15.0 mM) after addition of different amounts of CsOH: (a) 2.00, (b) 1.75, (c) 1.50, (d) 1.25, (e) 1.00, (f) 0.75, (g) 0.50, (h) 0.25, and (i) 0.00 equiv. Spectrum "a" corresponds to trimer B, and spectrum "i" corresponds to monomer A. The solvent peak is denoted by an asterisk (∗).
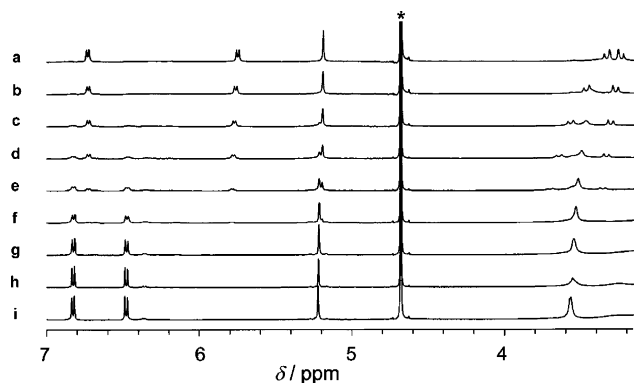
also seem to be of importance, as evidenced by the unusual behavior of the ester-substituted ruthenium complex, **4**.

Additional evidence for the presence of trimeric macrocycles at pH 8 was obtained by ESI mass spectrometry; spectra of solutions containing ligand **L1** and metal complex **3** or **10** showed isotopically resolved peaks for the monoprotonated trimers.

NMR titration experiments with mixtures, which display a $pK_a > 6$, gave slightly different results since more than 1 equiv of CsOH, with respect to the ligand, was needed to complete the assembly process. The amount of CsOH that was required to generate the metallamacrocycle was found to depend on the nature of the metal complex and the ligand. Whereas for a combination of ligand **L3** with (cymene)Ru complex **3**, the addition of 1.25 equiv of CsOH was sufficient to obtain over 95% of the respective trimer, almost 2 equiv of CsOH was needed for $(C_5Me_4H)Rh$ complex **8** (Figure 7). For some other mixtures, such as Cp*Rh complex **8** and ligand **L3**, precipitation was observed before completion of macrocyclization.

For the above-mentioned cases, the pyridone proton has an acidity comparable to that of the ammonium side chain.

Scheme 4
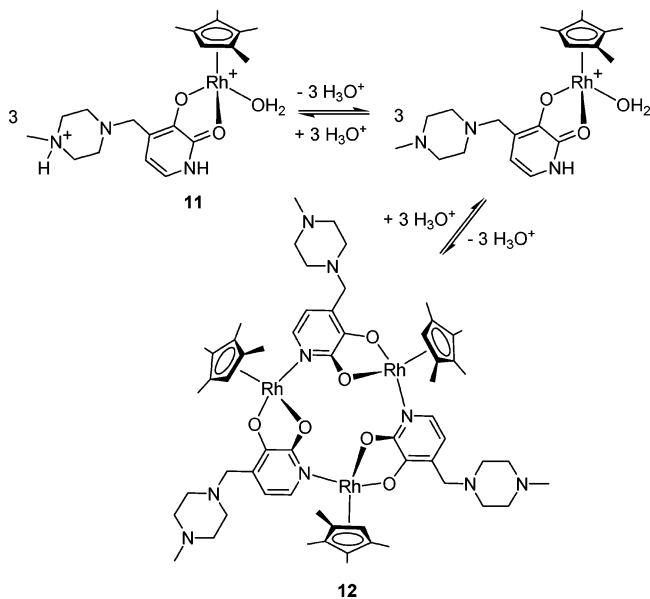
Accordingly, we observe the partial deprotonation of the side chain before the deprotonation of the pyridone. Since macrocyclization necessitates the deprotonation of the pyridone NH proton, more than 1 equiv of CsOH is needed. For the extreme case of complex **7** and ligand **L3**, this situation is illustrated in Scheme 4. When chloro-bridged complex **7** is dissolved with 2 equiv of ligand **L3**, monomeric complex **11** is formed. Addition of base initially leads to a deprotonation of the side chain. The assembly process to generate macrocycle **12**, therefore, requires 2 equiv of base (with respect to the ligand).

Structural Investigations. To obtain structural information about monomeric complexes of type A, we have crystallized the reaction products of various metal−ligand combinations without the addition of base. Suited single crystals were obtained for reactions of $(C_6Me_6)Ru$ complex **5** with ligands **L1**, **L2**, and **L4**. The molecular structures of one enantiomer of the resulting complexes (**13**−**15**) in the crystal are depicted in Figure 8.

Overall, the molecular structures are very similar. The ligands are coordinated to the Ru atoms via the two pyridone *O*-atoms forming five-membered chelate rings. As suggested by NMR data, the ligands are in a zwitterionic form with a deprotonated 3-hydroxy group and an ammonium side chain. In all cases, the NH proton of the ammonium group displays a hydrogen bond to the chloride counterion. A second hydrogen bond can be observed between the chloride counterion and the pyridone NH proton of an adjacent, symmetry-related complex. As a result, we observe the dimerization of the two enantiomeric ruthenium complexes present in the crystal via hydrogen bonding to two chloride anions (Figure 9). This arrangement seems to be energetically quite stable because it is observed for all three complexes. Since the crystals were obtained from organic solvents, the second chloride is coordinated to the metal
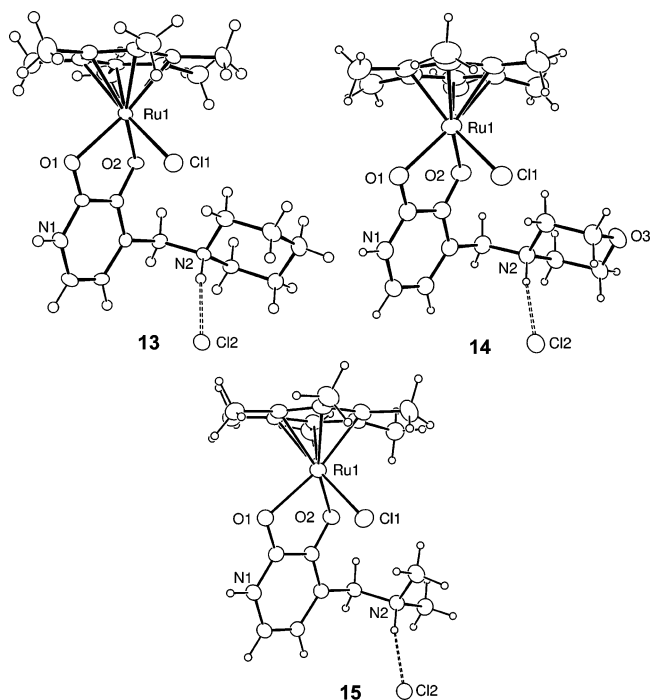

Figure 8. ORTEP[18] representations of the molecular structures of monomeric complexes **13**−**15** in the crystal. The complexes were obtained in reactions of the $(C_6Me_6)Ru$ complex **5** with 2 equiv of ligands **L1** (**13**), **L2** (**14**), or **L4** (**15**), respectively.
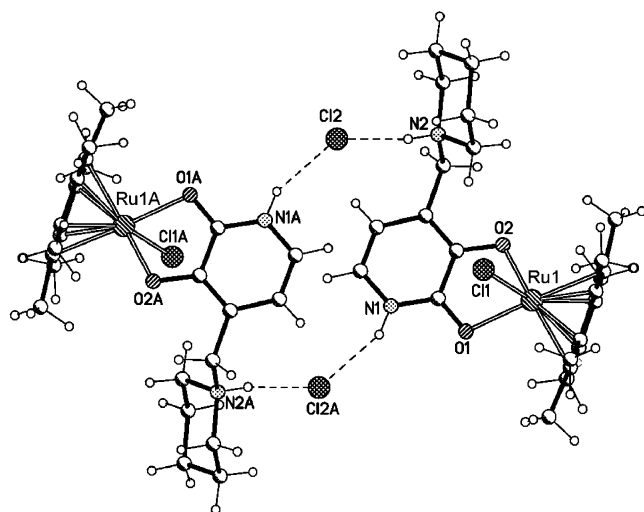
Figure 9. In the crystal, two cationic complexes **13** are connected via hydrogen bonding to the chloride counterions. A similar arrangement is found for complexes **14** and **15**.
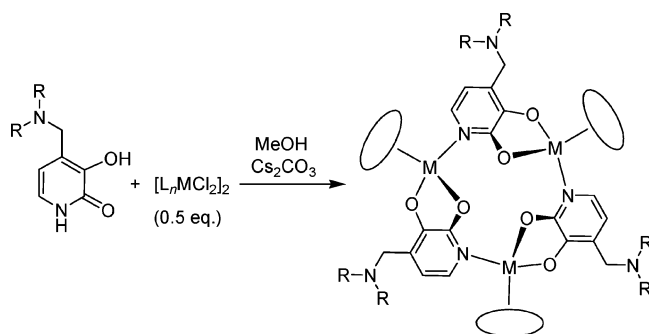
Table 2. Selected Bond Lengths (Å) and Angles (deg) of Monomeric Complexes **13**−**15**

	13	14	15
Ru1−Cl1	2.4198(10)	2.4295(16)	2.4328(17)
Ru1−O1	2.146(3)	2.170(4)	2.141(4)
Ru1−O2	2.085(3)	2.073(3)	2.080(3)
O1−Ru1−O2	78.58(10)	78.39(13)	78.32(13)
O1−Ru1−Cl1	83.30(8)	84.53(10)	85.16(11)
N2···Cl2	3.079(3)	3.070(4)	3.016(5)
N1···Cl2A	3.136(4)	3.166(4)	3.114(4)

and not replaced by an aqua-ligand. A summary of selected bond lengths and angles for the three complexes is given in Table 2.

Cationic complexes of type B were found to be difficult to crystallize, presumably due to the presence of three chloride counterions. We thus focused on the neutral, completely deprotonated complexes. They were obtained by reaction of the respective chloro-bridged complexes with 2 equiv of the pyridone ligands and an excess of base (Cs_2CO_3) in methanol (Scheme 5). After evaporation of the solvent, the products were separated from the salts by extraction with CH_2Cl_2 or hexane. Suited single crystals were obtained for complexes **16**−**19**.

Scheme 5

	(π-Ligand)M	Ligand
12	$(C_5Me_4H)Rh$	**L3**
16	(cymene)Ru	**L2**
17	(cymene)Ru	**L3**
18	Cp*Rh	**L3**
19	Cp*Ir	**L2**
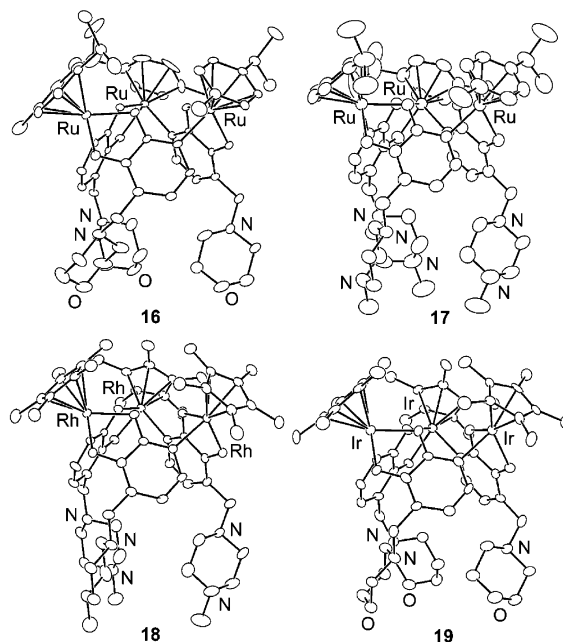
Figure 10. ORTEP representations of the molecular structures of complexes **16**−**19** in the crystal.

Table 3. Selected Bond Lengths (Å) and Angles (deg) for the Metallamacrocyclic Complexes Shown in Figure 10

	16[a]	17[a]	18	19
M−N1	2.141	2.142	2.130(2)	2.127(7)
M−O1	2.090	2.079	2.0949(19)	2.115(5)
M−O2	2.055	2.050	2.0546(19)	2.092(5)
O1−M−O2	79.06	79.50	80.09(8)	78.6(2)
O1···O1′	3.128	3.104	3.106(3)	3.040(8)
M···M′	5.369	5.342	5.353(1)	5.370(2)

[a] Averaged values are given.

Graphic representations of the molecular structures in the crystal are depicted in Figure 10.

All four complexes show the expected trinuclear metallamacrocyclic structure with the metal centers being bridged by the two adjacent *O*-atoms and the N-atom of the pyridonate ligand. A comparison of important structural parameters shows that the substitution of the (cymene)Ru fragment with a Cp*Ir or Cp*Rh fragment has only a small influence on the macrocyclic framework (Table 3).

A difference between the crystal structures of the Cp*M complexes on one side and the (cymene)Ru complexes on the other side is that for the latter, a water molecule can be found in the macrocyclic cavity.[19] These water molecules are within hydrogen bond distance to the bridging *O*-atoms (Figure 11). This is of special interest since the *O*-atoms represent the binding site for alkali metal ions (see below).

Host−Guest Chemistry. Macrocyclic complexes of type B (Scheme 3) can be regarded as organometallic analogues of 12-crown-3.[20] Similar to their organic counterparts,[21] they are able to bind lithium ions, although with a much higher affinity and selectivity (Scheme 6).

As reported in a recent communication,[13] the trimeric ruthenium complex, which is formed by reaction of complex **3** with ligand **L1** in buffered aqueous solution (100 mM phosphate buffer, pH 7.0), displays an association constant of $K_a = 2.3 \times$

Figure 11. View along the pseudo-C_3-symmetry axis of (cymene)Ru complex **16**, highlighting the hydrogen-bonded water molecules within the cavity of the macrocycle. Distances (Å): O1···O10 = 2.924(5); O4···O10 = 2.895(5); O7···O10 = 2.980(5).

Scheme 6

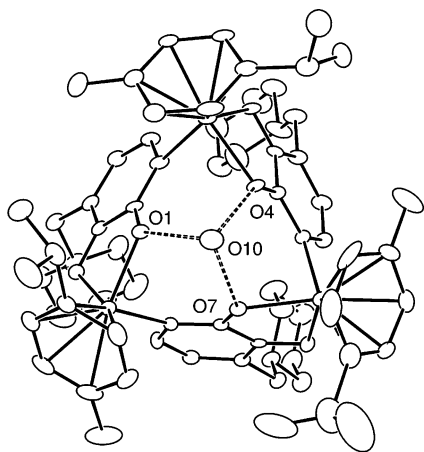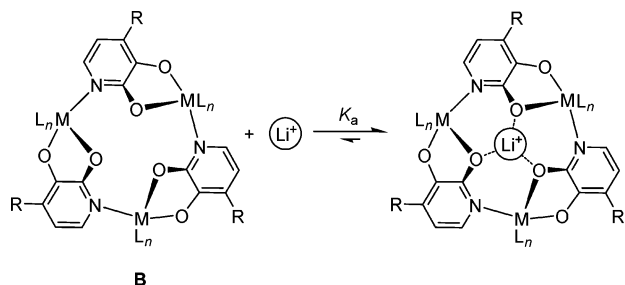10^3 M^{-1} for Li$^+$. A central point of the present study was to investigate how the affinity of these self-assembled receptors is influenced by structural modifications of the ligand and/or the metal fragment. We have therefore determined the Li$^+$ binding constants for several complexes of type B using the metal–ligand combinations specified in Table 4. The assembly process was induced in situ using CsOH. For all complexes, the binding constant was determined by ^{1}H NMR spectroscopy. The complexation of Li$^+$ results in pronounced differences in chemical shifts, and the exchange of Li$^+$ is slow compared to the NMR time scale (for a representative example, see Figure 12). This allows K_a to be calculated directly by integration of suited signals.

First, the influence of the different metal fragments was investigated using ligand **L1** (entries 1–9). For ruthenium complexes **1**–**4**, the data suggest a correlation between the electronic properties of the arene π-ligand and the association constant K_a. The lowest value of K_a (28($\pm$6) M^{-1}) is found for ($C_6H_5CO_2Et$)Ru complex **4**, having an electron-withdrawing ester substituent (entry 4). For (arene)Ru complexes **1**–**3**, the binding constants increase with the number of the electron-

(18) *ORTEP 3 for Windows*, version 1.074; Farrugia, L. J. *J. Appl. Crystallogr.* **1997**, *30*, 565.
(19) The hydrogen atoms could not be localized, presumably due to a rotational disorder along the pseudo-C_3-symmetry axis.
(20) For reviews on metallacrown complexes, see: (a) Pecoraro, V. L.; Stemmler, A. J.; Gibney, B. R.; Bodwin, J. J.; Wang, H.; Kampf, J. W.; Barwinski, A. In *Progress in Inorganic Chemistry*; Karlin, K., Ed.; Pergamon Press: New York, 1997; Vol. 45, pp 83–177. (b) Bodwin, J. J.; Cutland, A. D.; Malkani, R. G.; Pecoraro, V. L. *Coord. Chem. Rev.* **2001**, *216–217*, 489–512.
(21) (a) Fredriksen, S. B.; Dale, J. *Acta Chem. Scand.* **1992**, *46*, 1188–1194. (b) Dale, J.; Eggestad, J.; Fredriksen, S. B.; Groth, P. *J. Chem. Soc., Chem. Commun.* **1987**, 1391–1393.

Table 4. Binding Constants, K_a, for the Complexation of Li$^+$ and Na$^+$ of Selected Trinuclear Macrocycles[a]

entry	complex	ligand	equiv of CsOH[b]	equiv of MX[c]	K_a (M^{-1})
1	**1**	**L1**	1.0	2.0 LiCl	7.5($\pm$0.6) $\times$ 10^2
2	**2**	**L1**	1.0	2.0 (4.0) LiCl[d]	1.2($\pm$0.6) $\times$ 10^3
3	**3**	**L1**	1.0	2.0 LiCl	2.1($\pm$0.6) $\times$ 10^3
4	**4**	**L1**	1.0	4.0 (6.0) LiCl[d]	2.8($\pm$0.6) $\times$ 10^1
5	**6**	**L1**	1.0	2.0 (4.0) LiCl[d]	2.9($\pm$0.5) $\times$ 10^2
6	**7**	**L1**	1.5	2.0 LiCl	1.3($\pm$0.2) $\times$ 10^4
7	**8**	**L1**	1.3	50 Li$_2$SO$_4$	1.3($\pm$0.4) $\times$ 10^1
8	**9**	**L1**	1.0	2.0 (4.0) LiCl[d]	2.6($\pm$0.5) $\times$ 10^2
9	**10**	**L1**	1.0	50 Li$_2$SO$_4$	9.0($\pm$2.0) $\times$ 10^{-2}
10	**3**	**L2**	1.0	2.0 LiCl	2.3($\pm$0.6) $\times$ 10^3
11	**3**	**L4**	1.0	2.0 LiCl	2.4($\pm$0.6) $\times$ 10^3
12	**1**	**L3**	1.0	2.0 LiCl	4.0($\pm$0.6) $\times$ 10^3
13	**9**	**L3**	1.0	2.0 LiCl	1.2($\pm$0.6) $\times$ 10^3
14	**2**	**L3**	1.0	2.0 LiCl	5.4($\pm$0.5) $\times$ 10^3
15	**2**	**L3**	1.5	2.0 LiCl	1.3($\pm$0.5) $\times$ 10^4
16	**2**	**L3**	2.0	2.0 LiCl	3.0($\pm$0.6) $\times$ 10^4
17	**7**	**L3**	2.0	2.0 LiCl	5.6($\pm$2.1) $\times$ 10^4
18	**3**	**L3**	2.0	2.0 LiCl	5.8($\pm$1.0) $\times$ 10^4
19	**6**	**L1**	1.5	2.0 LiCl[c]	1.6($\pm$0.5) $\times$ 10^3
20	**3**	**L1**	1.0	1.0 Li$_2$SO$_4$	2.2($\pm$0.6) $\times$ 10^3
21	**3**	**L1**	1.0	2.0 LiNO$_3$	2.3($\pm$0.6) $\times$ 10^3
22	**3**	**L1**	1.0	2.0 LiOAc	2.2($\pm$0.6) $\times$ 10^3
23	**3**	**L1**	1.0	50 Na$_2$SO$_4$	5.0($\pm$1.0) $\times$ 10^{-1}
24	**7**	**L1**	1.5	50 Na$_2$SO$_4$	1.3($\pm$0.3)
25	**3**	**L2**	1.0	50 Na$_2$SO$_4$	6.0($\pm$1.0) $\times$ 10^{-1}
26	**3**	**L3**	2.0	15 (25) Na$_2$SO$_4$[d]	5.0($\pm$1.0)
27	**3**	**L4**	1.0	50 Na$_2$SO$_4$	6.0($\pm$1.0) $\times$ 10^{-1}
28	**7**	**L3**	2.0	15 (25) Na$_2$SO$_4$[d]	7.0($\pm$1.0)

[a] Binding constants were determined by ^{1}H NMR spectroscopy at receptor concentrations of 1.0 or 5.0 mM for Li$^+$ and Na$^+$, respectively. [b] Equivalents with respect to the amount of ligand. [c] Equivalents with respect to the amount of receptor formed. [d] Two different MX concentrations were employed to determine K_a.
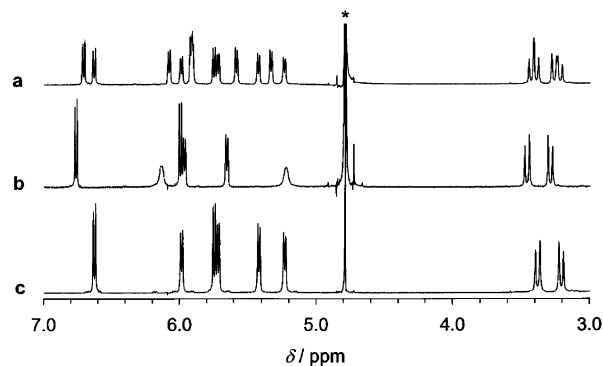
Figure 12. Part of the ^{1}H NMR spectrum (D$_2$O) of a solution containing receptor **17** (5.0 mM) and (a) Na$_2$SO$_4$ (125 mM), (b) LiCl (10.0 mM), or (c) no alkali metal salt. The addition of LiCl results in quantitative adduct formation, whereas for Na$_2$SO$_4$, a mixture between the free and the complexed receptor can be observed.

donating alkyl groups from K_a = 7.5($\pm$0.6) $\times$ 10^2 to 2.1($\pm$6) $\times$ 10^3 M^{-1} (entries 1–3). Similarly, (C_5Me_4H)Rh complex **7** displays an affinity for Li$^+$ (K_a = 1.3($\pm$0.2) $\times$ 10^4 M^{-1}) higher than that for CpRh complex **6** (K_a = 2.9($\pm$0.5) $\times$ 10^3 M^{-1}, entries 5 and 6). For Cp*Rh complex **8**, on the other hand, a relatively low binding constant of K_a = 1.3($\pm$0.4) $\times$ 10^1 M^{-1} was observed (entry 7). Here, the negative effect of the sterically demanding Cp* ligands, which block the binding site, dominates over the positive electronic effect of the five methyl groups on the Cp ligand.

The nature of the metal ion is a second important factor influencing the binding constants. Rhodium complexes were found to display higher binding constants than their analogous

iridium complexes (entry 6 vs 8; entry 7 vs 9). It is known that the polarity of the metal−oxygen bond is a crucial factor for the binding affinity of metallacrown complexes,[11b] and the observed difference between rhodium and iridium can possibly be attributed to a less-polar binding site (oxygen atoms) in the case of iridium receptors.

Macrocycles containing ligands **L1**, **L2**, and **L4** showed very similar affinities for Li$^+$ (entries 3, 10, and 11). Receptors based on ligand **L3**, on the other hand, displayed higher binding constants (entry 1 vs 12; entry 2 vs 14; entry 8 vs 13). As described above, a unique feature of ligand **L3** is that the protons are located on the terminal methylamino groups and not on the amino group adjacent to the pyridone. This means that the protons, and thus the positive charges, are located further away from the Li$^+$ binding site, which increases the affinity.

The importance of the charges prompted us to investigate the effect of the pH on the binding constants. The addition of more than 1 equiv of CsOH with respect to the ligand was expected to lead to a deprotonation of the amino side chains and, therefore, to a higher affinity for Li$^+$. This was indeed the case; if 1 equiv of CsOH was added to a mixture of ruthenium complex **2** and ligand **L3**, a binding constant of $K_a = 5.4(\pm0.5) \times 10^3 \text{ M}^{-1}$ was determined.[22] This value increased to $K_a = 1.3(\pm0.5) \times 10^4 \text{ M}^{-1}$ and finally to $K_a = 3.0(\pm0.6) \times 10^4 \text{ M}^{-1}$ upon addition of 1.5 or 2.0 equiv of CsOH, respectively (entries 14−16). A similar trend was observed for rhodium complex **6** in combination with **L1** (entries 5 and 19). These studies were restricted to metal−ligand combinations for which complete deprotonation did not result in precipitation.

Overall, the best Li$^+$ receptors were the macrocycles obtained from a combination of ligand **L3** with (cymene)Ru complex **3** ($K_a = 5.8(\pm1.0) \times 10^4 \text{ M}^{-1}$) or (C$_5Me_4$H)Rh complex **7** ($K_a = 5.6(\pm2.1) \times 10^4 \text{ M}^{-1}$) with 2 equiv of CsOH (entries 17 and 18). It should be noted that these values are among the highest ever reported for Li$^+$ complexation in water.[5] For potential applications, the ruthenium complex is particularly appealing because the starting material **3** is commercially available. The corresponding receptor **17** can either be prepared in situ by base-induced self-assembly or be synthesized prior to binding studies, as outlined in Scheme 5.[23]

In organic solvents, 12-metallacrown-3 complexes were found to bind lithium and sodium salts as ion pairs.[12] Consequently, the binding constants depend on the nature of the anion. For our water-soluble receptors, a dependence of this kind was not observed; the binding constants for the complexation of LiCl, Li$_2$SO$_4$, LiNO$_3$, and LiOAc were, within the limits of accuracy, all the same (entries 1 and 20−22).

A remarkable feature of the new receptors is their extremely high selectivity for Li$^+$ over Na$^+$. For most metal−ligand combinations, it was not possible to observe a complexation of Na$^+$ under the conditions employed ([receptor] = 5.0 mM, [Na$^+$] $\leq$ 500 mM). Only for the high-affinity receptors formed from **3** and **7** was it possible to observe Na$^+$ adducts by ^{1}H NMR spectroscopy and thus to calculate the binding constants. As listed in Table 4, the values for the complexation of Na$^+$
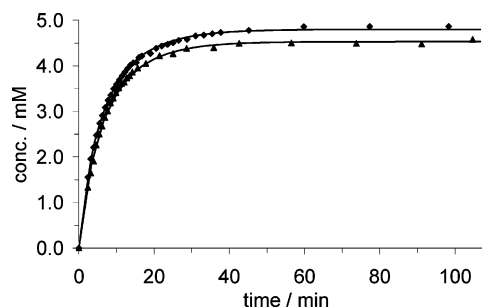

Figure 13. Time course of Li$^+$ adduct formation of the receptor obtained from **3**, **L1**, and 1 equiv of CsOH (▲) and of receptor **17** (◆), as determined by ^{1}H NMR spectroscopy (D$_2$O; [Li$^+$] = 9.8 mM; [receptor] = 4.9 mM).

are approximately 4 orders of magnitude lower than the values determined for Li$^+$ (entries 23−28).

To obtain more information about the differences of the high-affinity host **17** and the cationic host obtained from **3**, **L1**, and 1.0 equiv of CsOH (entry 3), we have investigated the kinetics of Li$^+$ complexation. A stock solution of LiCl (final [Li$^+$] = 10 mM) was added to a solution of the respective receptor in D$_2$O (4.9 mM). The time course of adduct formation was then determined by ^{1}H NMR spectroscopy. The results are depicted in Figure 13. Fitting of the experimental data to a simple bimolecular reaction model[24] showed that the complexation rates (k_{on}) for both receptors are very similar; for the combination of **3** and **L1**, a value of $2.72(\pm0.02) \times 10^{-4} \text{ mM}^{-1} \text{ s}^{-1}$ was determined, whereas for **17**, a value of $2.94(\pm0.03) \times 10^{-4} \text{ mM}^{-1} \text{ s}^{-1}$ was found. The difference in affinity can therefore be attributed to a difference in the decomplexation rates (k_{off}) of the two hosts. For **3**/**L1**/1 equiv of CsOH, a value of $k_{off} = 1.17(\pm0.05) \times 10^{-4} \text{ s}^{-1}$ was determined. The resulting calculated binding constant of $K_a = k_{on}/k_{off} = 2.3 \times 10^3 \text{ M}^{-1}$ corresponds well to that determined by ^{1}H NMR spectroscopy under equilibrium conditions (Table 4, entry 3). For the high-affinity receptor **17**, a meaningful decomplexation rate could not be deduced from the kinetic data because, by ^{1}H NMR, we observed the quantitative formation of the Li$^+$ adduct under the conditions employed. Using the value for the binding constant determined at a lower receptor concentration of 1.0 mM (Table 4, entry 18), however, a decomplexation rate, $k_{off} = 5 \times 10^{-6}$ s^{-1} can be estimated.

The base-induced macrocyclization of **3** and **L3** to give receptor **17** was found to be a reversible process; when 6 equiv of DCl was added to a solution of **17** in D$_2$O, the spectrum of the monomeric complex, [(cymene)Ru(**L3**)OH$_2$]$^+$, was observed by ^{1}H NMR spectroscopy (Scheme 7). Accordingly, a potentiometric titration of **17** with HCl gave a curve, which was nearly identical with that found for **3**, **L3**, and CsOH (Figure 14).[25] In the presence of LiCl, however, a different behavior was observed. Addition of HCl to a solution of **17** containing lithium ions resulted in the immediate protonation of the amine side chains but not in the cleavage of the macrocycle (Scheme 7). This is reflected by the titration curves with HCl; the first part is identical for titrations with and without Li$^+$, but after addition

(22) With only 1 equiv of CsOH, the macrocyclization was not quantitative, and 10% of a monomeric complex of type A was observed. For the calculation of the binding constant, the concentrations were adjusted accordingly.

(23) The Li$^+$ binding constant of **17** was found to be identical to that of the in situ generated receptor.

(24) The kinetic data were fitted with the help of the Gepasi program, version 3.30, using a preinstalled Levenberg−Marquardt algorithm: (a) Mendes, P. *Comput. Appl. Biosci.* **1993**, *9*, 563−571. (b) Mendes, P. *Trends Biochem. Sci.* **1997**, *22*, 361−363.

(25) Small deviations with respect to the reverse titration curve with CsOH are observed in the final part of the curve (5−6 equiv of HCl). They can be reduced if the titrations are performed very slowly.
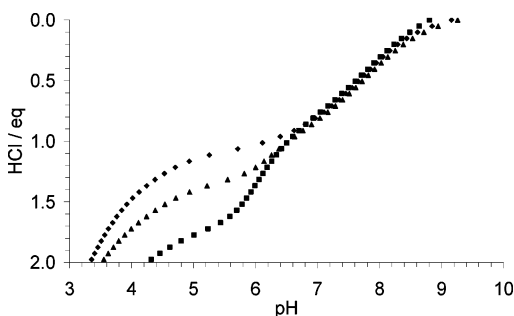
Figure 14. The pH of solutions containing receptor **17** (5.0 mM) after addition of increasing amounts of HCl. The titrations were performed in the presence of 1.0 equiv of LiCl (◆), 0.5 equiv LiCl (▲), and without LiCl (■).
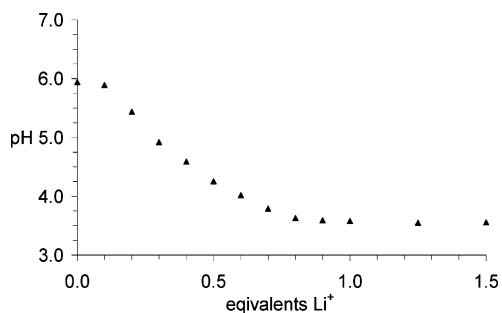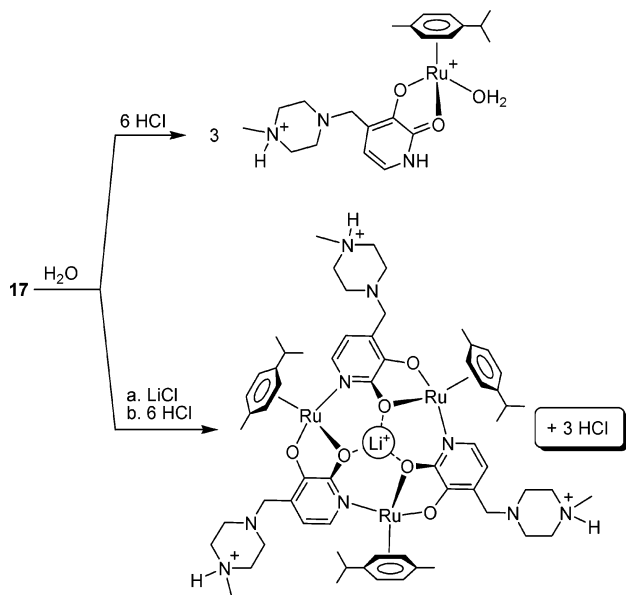

Figure 15. The pH of solutions containing receptor **17** (5.0 mM) in the presence of various amounts of LiCl (0−1.5 equiv) after addition of HCl (4.5 equiv, with respect to the receptor).

Scheme 7

of 3 equiv of HCl, we observe a sharp drop in pH for solutions containing Li$^+$ because the acid is not consumed to form monomeric complexes (Figure 14).

The different behavior of receptor **17** in the presence and absence of lithium ions offers the possibility to detect Li$^+$ in water by a simple pH measurement. Various amounts of Li$^+$ (0−1.5 equiv, with respect to the receptor) were added to a solution of receptor **17** (5.0 mM). After equilibration, 4.5 equiv of HCl was added, and the pH was determined (Figure 15). Between 0 and 1.0 equiv of Li$^+$, the resulting pH differs by more than 2 units. This difference is sufficient to allow a semiquantitative determination of Li$^+$ in the low millimolar
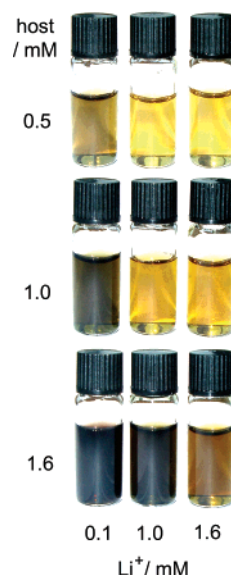
Figure 16. Photos of aqueous solutions containing different concentrations of host **17** (0.5, 1.0, and 1.6 mM) and different lithium concentrations (0.1, 1.0, and 1.6 mM) after addition of an excess of FeCl$_3$ (3 equiv, with respect to **17**). A brown color is observed for solutions in which receptor **17** is not saturated with Li$^+$. The photos were recorded 1 min after addition of FeCl$_3$.

concentration range using commercially available pH strips (accuracy of 0.5 pH units).

From the reactions with HCl, it was apparent that the kinetic and thermodynamic stability of receptor **17** was enhanced in the presence of lithium ions. This prompted us to investigate whether a difference between the free receptor **17** and the host−guest complex [**17**·Li$^+$] can also be observed for other chemical reactions. Screening of a number of different reagents revealed that simple Fe(III) salts are ideally suited; when an excess of FeCl$_3$ was added to an aqueous solution of **17**, the receptor immediately decomposed to give a dark-brown solution from which a brown powder slowly precipitated.[26] In the presence of lithium ions, this reaction was kinetically inhibited, and addition of FeCl$_3$ lead to no immediate color change.[27] This difference in reactivity can be used for the "naked eye" detection of Li$^+$ in water in the pharmacologically relevant concentration range of 0.5−1.5 mM.[5] An example is shown in Figure 16. Nine solutions with three different receptor concentrations (0.5, 1.0, and 1.6 mM) and three different Li$^+$ concentrations (0.1, 1.0, and 1.6 mM) were prepared. Upon addition of an excess of FeCl$_3$ (∼3 equiv, with respect to **17**), a color change was only observed for solutions in which the receptor was not saturated with Li$^+$. A 3 × 3 assay of this kind can thus be used to determine if the Li$^+$ concentration is in the range of 0−0.5, 0.5−1.0, 1.0−1.5, or above 1.5 mM. It remains to be seen whether a colorimetric test of this kind can be used to determine Li$^+$ in more complicated matrixes, such as body fluids. From previous studies, it is known that peptides may show a high affinity to half-sandwich complexes of Rh(II) and Rh(III).[28] It therefore seems likely that peptides would have to be removed from the sample prior to testing.

(26) Attempts to identify the product of the reaction between **17** and FeCl$_3$ were not successful.
(27) After 30 min, a dark precipitate was also observed in the presence of lithium ions.

Conclusion

The utilization of assembly processes to build artificial receptors[29] or chemosensors[30] is conceptually very appealing, given that the building blocks are easily accessible. We have shown that potent receptors for the pharmacologically interesting lithium ion can be obtained by base-induced assembly of half-sandwich complexes with simple 3-hydroxy-2-pyridone derivatives. Due to the inherent flexibility of this approach, it was possible to investigate the host–guest chemistry of a large variety of receptors in relatively short time. Of all receptors tested, ruthenium complex **17** displayed the most interesting characteristics. In water, it shows a Li$^+$ binding constant of K_a = 5.8($\pm$1.0) $\times$ 10^4 M^{-1}. This value is among the highest ever reported for Li$^+$ complexation in water,[5] and it is sufficient for the quantitative complexation of Li$^+$ in the pharmacologically relevant concentration range of $\sim$1 mM. The selectivity of **17** is extremely high; the complexation of K$^+$ or Cs$^+$ could not be detected at all, and its affinity for Na$^+$ is 4 orders of magnitude lower than that for Li$^+$. To use receptor **17** for sensing, two methods to transduce the binding event into a signal output were developed. This first is based on the Li$^+$-induced stabilization of **17** against deaggregation by acid and allows the detection of low millimolar concentrations of Li$^+$ by a change in pH. The second is based on the differential reactivity of **17** and its lithium adduct, [**17**·Li$^+$], toward FeCl$_3$. Since this reaction is accompanied by a strong change of color, it is possible to detect Li$^+$ at concentrations of $\sim$1 mM by the "naked eye". For potential applications, it is of importance that receptor **17** can be synthesized in situ by self-assembly, using the commercially available complex **3** and a pyridone ligand **L3**, which is accessible in a one-step procedure.

Experimental Section

General. Complexes [(C$_6$H$_6$)RuCl$_2$]$_2$ (**1**),[31] [(C$_6$H$_5$Me)RuCl$_2$]$_2$ (**2**),[32] [(cymene)RuCl$_2$]$_2$ (**3**),[33] [(C$_6$H$_5$CO$_2$Et)RuCl$_2$]$_2$ (**4**),[34] [(C$_6$Me$_6$)RuCl$_2$]$_2$ (**5**),[33] [(C$_5$H$_5$)RhCl$_2$]$_2$ (**6**),[35] [(C$_5$Me$_4$H)RhCl$_2$]$_2$ (**7**),[36] [Cp*RhCl$_2$]$_2$ (**8**),[37] and [Cp*IrCl$_2$]$_2$ (**10**)[37] and ligands **L1**–**L4**[14] were prepared according to literature procedures. The synthesis of [(C$_5$Me$_4$H)IrCl$_2$]$_2$ (**9**) was performed analogously to that of **7**.[38] Cs$_2$CO$_3$ (99.9%) was purchased

(28) (a) Buryak, A.; Severin, K. *Angew. Chem., Int. Ed.* **2004**, *43*, 4771–4774. (b) McNae, I. W.; Fishburne, K.; Habtemariam, A.; Hunter, T. M.; Melchart, M.; Wang, F.; Walkinshaw, M. D.; Sadler, P. J. *Chem. Commun.* **2004**, 1786–1787. (c) Severin, K.; Bergs, R.; Beck, W. *Angew. Chem., Int. Ed.* **1998**, *37*, 1635–1654.

(29) For some examples of self-assembled receptors for alkali metal ions, see: (a) Davis, J. T. *Angew. Chem., Int. Ed.* **2004**, *43*, 668–698. (b) Nabeshima, T.; Takahashi, T.; Hanami, T.; Kikuchi, A.; Kawabe, T.; Yano, Y. *J. Org. Chem.* **1998**, *63*, 3802–3803. (c) Rudkevich, D. M.; Shivanyuk, A. N.; Brzozka, Z.; Verboom, W.; Reinhoudt, D. N. *Angew. Chem., Int. Ed. Engl.* **1995**, *34*, 2124–2126. (d) Schepartz, A.; McDevitt, J. P. *J. Am. Chem. Soc.* **1989**, *111*, 5976–5977.

(30) For the construction of chemosensors via noncovalent interactions, see: (a) Wiskur, S. L.; Aït-Haddou, H.; Lavigne, J. J.; Anslyn, E. V. *Acc. Chem. Res.* **2001**, *34*, 963–972. (b) Fabbrizzi, L.; Licchelli, M.; Taglietti, A. *Dalton Trans.* **2003**, 3471–3479. (c) Sukasai, C.; Tuntulani, T. *Chem. Soc. Rev.* **2003**, *32*, 192–202.

(31) Zelonka, R. A.; Baird, M. C. *Can. J. Chem.* **1972**, *50*, 3063–3072.

(32) Bennett, M. A.; Smith, A. K. *J. Chem. Soc., Dalton Trans.* **1974**, *2*, 234–241.

(33) Bennett, M. A.; Huang, T.-N.; Matheson, T. W.; Smith, A. K. *Inorg. Synth.* **1982**, *21*, 74–78.

(34) Therrien, B.; Ward, T. R.; Pilkington, M.; Hoffmann, C.; Gilardoni, F.; Weber, J. *Organometallics* **1998**, *17*, 330–337.

(35) Kang, J. W.; Moseley, K.; Maitlis, P. M. *J. Am. Chem. Soc.* **1969**, *91*, 5970–5977.

(36) Bellabarba, R.; Nieuwenhuyzen, M.; Saunders, G. C. *Inorg. Chim. Acta* **2001**, *323*, 78–88.

(37) White, C.; Yates, A.; Maitlis, P. M. *Inorg. Synth.* **1992**, *29*, 228–234.

(38) Contrary to what was reported by Werner et al., complex **7** could be obtained by reaction of IrCl$_3$·3H$_2$O and tetramethylcyclopentadiene: Mahr, A.; Nürnberg, O.; Werner, H. *Z. Anorg. Allg. Chem.* **2003**, *629*, 91–98.

from Aldrich, and 3-hydroxy-2-pyridone was purchased from Lancaster. All reactions, except the potentiometric titrations and the colorimetric tests, were carried out under an atmosphere of dry nitrogen using standard Schlenck techniques. It should be noted, however, that the macrocycles are not very air-sensitive; aqueous solutions of the receptors can be handled in air for several hours without significant decomposition. The ^{1}H and ^{13}C spectra were recorded on a Bruker Avance DPX 400 spectrometer using the residual protonated solvents (^{1}H, ^{13}C) as internal standards or LiCl in water as an external standard. All spectra were recorded at room temperature. Potentiometric titrations were carried out using a Metrohm Titrino 716 DMS instrument. The MS studies were performed with solutions of the respective macrocycle in water/acetonitrile (3:1) containing 50 mM phosphate buffer (pH $\sim$8).

General Procedure for the Synthesis of Monomeric Complexes in Water: The half-sandwich complex [(π-ligand)MCl$_2$]$_2$ (37.5 μmol) and the ligand (75.0 μmol) were stirred in water (5.00 mL) until a clear solution was obtained.

General Procedure for the Synthesis of Monomeric Complexes 13–15: A mixture of [(C$_6$Me$_6$)RuCl$_2$]$_2$ (**5**) (75.0 μmol, 50.0 mg) and the corresponding ligand (150 μmol) was stirred in chloroform or dichloromethane (20 mL) for 15 min. Evaporation of the solvent under reduced pressure gave the product in quantitative yield.

[(C$_6$Me$_6$)Ru(L1)Cl]Cl (13): Crystals were obtained by slow diffusion of ether into a solution of **13** in dichloromethane. ^{1}H NMR (400 MHz, D$_2$O): δ 1.30–2.30 (m, br, 6H, CH$_2$, piperidine), 2.14 (s, 18H, C$_6$Me$_6$), 3.04 (m, br, 2H, NCH$_2$, piperidine), 3.50 (m, br, 2H, piperidene), 4.21 (s, 2H, NCH$_2$), 6.46 (d, ^3J = 7 Hz, 1H, CH, pyridone), 6.82 (d, ^3J = 7 Hz, 1H, CH, pyridone). ^{13}C NMR (101 MHz, D$_2$O): δ 17.86 (CH$_3$, C$_6$Me$_6$), 23.92, 25.80, (CH$_2$, piperidine), 56.15, 57.42 (NCH$_2$), 91.79 (C$_6$Me$_6$), 117.02, 121.56, 123.48, 161.41, 167.58 (pyridone). Elemental analysis (%) calcd (found) for C$_{23}$H$_{34}$Cl$_2$N$_2$O$_2$-Ru·0.5CH$_2$Cl$_2$: C, 48.25 (48.88); H, 6.03 (6.08); N, 4.79 (4.42).

[(C$_6$Me$_6$)Ru(L2)Cl]Cl (14): Crystals were obtained by slow diffusion of pentane into a solution of **14** in chloroform. ^{1}H NMR (400 MHz, D$_2$O): δ 2.13 (s, 18H, C$_6$Me$_6$), 3.34 (m, br, 4H, NCH$_2$, morpholine), 3.93 (m, br, 4H, OCH$_2$, morpholine), 4.27 (s, 2H, NCH$_2$), 6.46 (d, ^3J = 7 Hz, 1H, CH, pyridone), 6.81 (d, ^3J = 7 Hz, 1H, CH, pyridone). ^{13}C NMR (101 MHz, D$_2$O): δ 17.87 (CH$_3$, C$_6$Me$_6$), 54.54, 57.50, 66.77 (NCH$_2$, OCH$_2$), 91.81 (C$_6$Me$_6$), 116.99, 121.39, 128.55, 161.73, 167.68 (pyridone). Elemental analysis (%) calcd (found) for C$_{22}$H$_{32}$Cl$_2$N$_2$O$_6$Ru·0.5CHCl$_3$: C, 44.73 (44.43); H, 5.42 (5.29); N, 4.64 (4.44).

[(C$_6$Me$_6$)Ru(L4)Cl]Cl (15): Crystals were obtained by slow diffusion of pentane into a solution of **15** in chloroform. ^{1}H NMR (400 MHz, D$_2$O): δ 2.14 (s, 18H, C$_6$Me$_6$), 2.90 (s, 6H, NMe$_2$), 4.27 (s, 2H, NCH$_2$), 6.46 (d, ^3J = 7 Hz, 1H, CH, pyridone), 6.82 (d, ^3J = 7 Hz, 1H, CH, pyridone). ^{13}C NMR (101 MHz, D$_2$O): δ 17.84 (CH$_3$, C$_6$Me$_6$), 45.49, 58.54 (NMe$_2$, NCH$_2$), 91.83 (C$_6$Me$_6$), 116.44, 121.46, 123.59, 161.45, 167.61 (pyridone). Elemental analysis (%) calcd (found) for C$_{20}$H$_{30}$Cl$_2$N$_2$O$_2$Ru·0.5CHCl$_3$: C, 43.80 (44.43); H, 5.47 (5.73); N, 4.98 (5.22).

[(C$_5$Me$_4$H)Rh(L3-2H$^+$)]$_3$ (12): A suspension of complex **7** (295 mg, 0.50 mmol), ligand **L3** (223 mg, 1.00 mmol), and Cs$_2$CO$_3$ (815 mg, 2.50 mmol) in degassed methanol (30 mL) was stirred for 2 h at room temperature. After evaporation of the solvent under reduced pressure, the product was extracted with dichloromethane (40 mL). After addition of hexane (60 mL) and evaporation of the solvent, a red-brown powder was obtained, which was dried in a vacuum (yield: 348 mg, 64%). ^{1}H NMR (400 MHz, CDCl$_3$): δ 1.44 (s, 9H, CH$_3$), 1.53 (s, 9H, CH$_3$), 1.67 (s, 9H, CH$_3$), 1.86 (s, 9H, CH$_3$), 2.00–2.75 (m, br, 24H, CH$_2$, piperazine), 2.25 (s, 9H, NCH$_3$, piperazine), 3.24 (d, ^2J = 13 Hz, 3H, NCH$_2$), 3.43 (d, ^2J = 13 Hz, 3H, NCH$_2$), 5.04 (s, 3H, Me$_4$C$_5$H), 5.75 (d, ^3J = 6 Hz, 3H, CH, pyridone), 6.57 (d, ^3J = 6 Hz, 3H, CH, pyridone). ^{13}C NMR (101 MHz, CDCl$_3$): δ 11.21, 11.43, 13.20, 13.37 (CH$_3$, Me$_4$C$_5$H), 49.07 (NCH$_3$), 56.20, 58.30, 58.63 (NCH$_2$, piperazine), 76.80 (d, $^1J_{C-Rh}$ = 8 Hz, CH, Me$_4$C$_5$H), 97.34 (d, $^1J_{C-Rh}$ = 6 Hz, C,

Me$_4$C$_5$H), 102.68 (d, $^1J_{C-Rh}$ = 6 Hz, C, Me$_4$C$_5$H), 115.40, 125.34, 132.54, 159.38, 172.85 (pyridone). Elemental analysis (%) calcd (found) for C$_{60}$H$_{84}$N$_9$O$_6$Rh$_3$·2H$_2$O·3CH$_2$Cl$_2$: C, 46.51 (46.46); H, 5.82 (5.97); N, 7.75 (7.71). During the NMR experiments with receptor **12**, we observed that the ^{1}H NMR signals of the methyl groups of the π-ligand gradually lost intensity. A likely explanation for this observation is a selective H/D exchange. An exchange of this kind has been observed for aqueous solutions of Cp*Rh[39] and Cp*Ru complexes.[40] A more detailed analysis revealed that the H/D exchange is slightly inhibited if the receptor is bound to a Li$^+$ guest; in the presence of 2 equiv of LiCl, 7% of the methyl protons were exchanged after 24 h, whereas without lithium ions, 20% were exchanged.

[(Cymene)Ru(L2-2H$^+$)]$_3$ (16): A suspension of complex **3** (306 mg, 0.50 mmol), ligand **L2** (210 mg, 1.00 mmol), and Cs$_2$CO$_3$ (815 mg, 2.50 mmol) in degassed methanol (20 mL) was stirred for 2 h at room temperature. After evaporation of the solvent under reduced pressure, the product was extracted with dichloromethane (40 mL). Twice the volume of hexane was added, and the solution was concentrated to 10 mL. The orange precipitate was isolated and dried in a vacuum (yield: 305 mg, 62%). Crystals were obtained by slow diffusion of pentane into a solution of **16** in benzene. ^{1}H NMR (400 MHz, CDCl$_3$): δ 1.28 (d, ^3J = 7 Hz, 9H, CH(C*H*$_3$)$_2$), 1.37 (d, ^3J = 7 Hz, 9H, CH(C*H*$_3$)$_2$), 2.12 (s, 9H, CH$_3$, C*H*$_3$C$_6$H$_4$^{i}Pr), 2.22 (m, br, 12H, CH$_2$, morpholine), 2.75 (sept, ^3J = 7 Hz, 3H, C*H*(CH$_3$)$_2$), 3.35 (d, ^2J = 14 Hz, 3H, NCH$_2$), 3.33 (d, ^2J = 14 Hz, 3H, NCH$_2$), 2.55 (m, br, 12H, CH$_2$, morpholine), 5.08 (d, ^3J = 6 Hz, 3H, MeC$_6$*H*$_4$^{i}Pr), 5.20 (d, ^3J = 6 Hz, 3H, MeC$_6$*H*$_4$^{i}Pr), 5.29 (d, ^3J = 6 Hz, 3H, MeC$_6$*H*$_4$^{i}Pr), 5.52 (d, ^3J = 6 Hz, 3H, MeC$_6$*H*$_4$^{i}Pr), 5.68 (d, ^3J = 6 Hz, 3H, CH, pyridone), 6.49 (d, ^3J = 6 Hz, 3H, CH, pyridone). ^{13}C NMR (101 MHz, CDCl$_3$): δ 18.60, 22.93, 23.20 (CH$_3$, MeC$_6$H$_4$^{i}Pr), 31.37 (CH, CH(CH$_3$)$_2$), 54.08, 55.71, 67.28 (NCH$_2$, OCH$_2$, morpholine), 77.36, 79.93, 81.49, 82.03 (CH, MeC$_6$H$_4$^{i}Pr), 95.80, 98.07 (C, MeC$_6$H$_4$^{i}Pr), 110.25, 123.11, 131.22, 155.32, 170.83 (pyridone). Elemental analysis (%) calcd (found) for C$_{60}$H$_{78}$N$_6$O$_9$Ru$_3$·H$_2$O·1.5CH$_2$Cl$_2$: C, 50.05 (50.37); H, 5.67 (6.06); N, 5.69 (5.44).

[(Cymene)Ru(L3-2H$^+$)]$_3$ (17): A suspension of complex **3** (612 mg, 1.00 mmol), ligand **L3** (447 mg, 2.00 mmol), and Cs$_2$CO$_3$ (1.60 g, 5.00 mmol) in degassed methanol (40 mL) was stirred for 2 h at room temperature. After evaporation of the solvent under reduced pressure, the product was extracted with hot hexane (1 × 300 mL and 3 × 125 mL). The solution was concentrated (15 mL) and stored at −18 °C for 1 h. The product precipitated as an orange powder, which was isolated and dried in a vacuum (yield: 502 mg, 54%). Crystals were obtained by slow diffusion of pentane into a solution of **17** in benzene. ^{1}H NMR (400 MHz, CDCl$_3$): δ 1.26 (d, ^3J = 7 Hz, 9H, CH(C*H*$_3$)$_2$), 1.34 (d, ^3J = 7 Hz, 9H, CH(C*H*$_3$)$_2$), 2.09 (s, 9H, C*H*$_3$C$_6$H$_4$^{i}Pr), 2.22 (s, 9H, NCH$_3$, piperazine), 1.75−2.65 (m, br, 24H, NCH$_2$, piperazine), 2.73 (sept, ^3J = 7 Hz, 3H, C*H*(CH$_3$)$_2$), 3.28 (d, ^2J = 13 Hz, 3H, NCH$_2$), 3.33 (d, ^2J = 13 Hz, 3H, NCH$_2$), 5.09 (d, ^3J = 5 Hz, 3H, MeC$_6$*H*$_4$^{i}Pr), 5.21 (d, ^3J = 6 Hz, 3H, MeC$_6$*H*$_4$^{i}Pr), 5.30 (d, ^3J = 6 Hz, 3H, MeC$_6$*H*$_4$^{i}Pr), 5.56 (d, ^3J = 5 Hz, 3H, MeC$_6$*H*$_4$^{i}Pr), 5.69 (d, ^3J = 6 Hz, 3H, CH, pyridone), 6.49 (d, ^3J = 6 Hz, 3H, CH, pyridone). ^{13}C NMR (101 MHz, CDCl$_3$): δ 18.86, 22.87, 23.19 (CH$_3$, MeC$_6$H$_4$^{i}Pr), 31.26 (CH, CH(CH$_3$)$_2$), 46.27 (NCH$_3$), 53.48, 55.27, 55.54 (NCH$_2$, piperazine), 77.32, 79.89, 81.53, 82.15 (CH, MeC$_6$H$_4$^{i}Pr), 95.97, 98.01 (C, cymene), 110.35, 123.96, 131.20, 154.99, 170.67 (pyridone). Elemental analysis (%) calcd (found) for C$_{63}$H$_{87}$N$_9$O$_6$Ru$_3$·H$_2$O: C, 54.53 (54.48); H, 6.46 (6.79); N, 9.08 (9.22).

[Cp*Rh(L3-2H$^+$)]$_3$ (18): A suspension of complex **8** (309 mg, 0.50 mmol), ligand **L3** (223 mg, 1.00 mmol), and Cs$_2$CO$_3$ (815 mg, 2.50 mmol) in degassed methanol (40 mL) was stirred for 2 h at room temperature. After evaporation of the solvent under reduced pressure, the product was extracted with dichloromethane (40 mL). Evaporation

of the solvent gave a red-brown powder, which was dried in a vacuum (yield: 325 mg, 55%). Crystals were obtained by slow diffusion of pentane into a solution of **18** in benzene. ^{1}H NMR (400 MHz, CDCl$_3$): δ 1.68 (s, 45H, CH$_3$, Cp*), 2.05−2.75 (m, br, 24H, NCH$_2$, piperazine), 2.25 (s, 9H, NCH$_3$, piperazine), 3.27 (d, ^2J = 13 Hz, 3H, NCH$_2$), 3.37 (d, ^2J = 13 Hz, 3H, NCH$_2$), 5.66 (d, ^3J = 6 Hz, 3H, CH, pyridone), 6.54 (d, ^3J = 6 Hz, 3H, CH, pyridone). ^{13}C NMR (101 MHz, CDCl$_3$): δ 9.31 (CH$_3$, Cp*), 46.30 (NCH$_3$), 53.43, 55.56, 55.92 (NCH$_2$, piperazine), 89.83 (d, $^1J_{C-Rh}$ = 8 Hz, C, Cp*), 111.45, 121.36, 130.11, 157.24, 170.53 (pyridone). Elemental analysis (%) calcd (found) for C$_{63}$H$_{87}$N$_9$O$_6$Ru$_3$·1.5CH$_2$Cl$_2$: C, 51.46 (51.26); H, 6.23 (6.24); N, 8.37 (8.31).

[Cp*Ir(L2-2H$^+$)]$_3$ (19): A suspension of complex **10** (398 mg, 0.50 mmol), ligand **L2** (210 mg, 1.00 mmol), and Cs$_2$CO$_3$ (815 mg, 2.50 mmol) in degassed methanol (40 mL) was stirred for 2 h at room temperature. After evaporation of the solvent under reduced pressure, the product was extracted with dichloromethane (40 mL). Evaporation of the solvent gave an orange powder, which was dried in a vacuum (yield: 321 mg, 59%). Crystals were obtained by slow diffusion of pentane into a solution of **19** in dichloromethane. ^{1}H NMR (400 MHz, CDCl$_3$): δ 1.65 (s, 45H, CH$_3$, Cp*), 2.35 (m, br, 12H, CH$_2$, morpholine), 3.34 (d, ^2J = 13 Hz, 3H, NCH$_2$), 3.39 (d, ^2J = 13 Hz, 3H, NCH$_2$), 3.63 (m, br, 12H, CH$_2$, morpholine), 5.67 (d, ^3J = 6 Hz, 3H, CH, pyridone), 6.59 (d, ^3J = 6 Hz, 3H, CH, pyridone). ^{13}C NMR (101 MHz, CDCl$_3$): δ 9.54 (CH$_3$, Cp*), 54.02, 56.07, 67.38 (CH$_2$, morpholine), 80.94 (C, Cp*), 111.59, 122.10, 130.51, 158.24, 172.55 (pyridone). Elemental analysis (%) calcd (found) for C$_{60}$H$_{81}$N$_6$O$_9$Ir$_3$·2H$_2$O: C, 43.86 (43.55); H, 5.21 (5.14); N, 5.12 (4.74).

General Procedure for the Determination of the Binding Constant K_a: In a typical experiment, a mixture of the half-sandwich complex [(π-ligand)MCl$_2$]$_2$ (37.5 μmol) and the respective ligand (75.0 μmol) was stirred in water (4.25 mL) until a clear solution was obtained. A 250 μL stock solution of CsOH (0.3 M) was added to induce the assembly process. The solution was divided into five equal parts (900 μL, 5.55 mM), and stock solutions of various alkali metal salts were added: LiCl (100 μL, 0.10 M), Na$_2$SO$_4$ (125 μL, 2.0 M), KOAc (125 μL, 4.0 M), CsOAc (125 μL, 4.0 M). The mixtures were equilibrated for 24 h at room temperature. The binding constants, K_a, were determined by integration of the ^{1}H NMR signals of the free and complexed receptor. In most cases, several baseline-separated signals were available, and averaged values were employed. The concentration of the receptor in such an experiment was 5.0 mM; the concentration of Li$^+$ was 10.0 mM (2.0 equiv), and the concentrations of Na$^+$, K$^+$, and Cs$^+$ were 500 mM (50 equiv). For experiments with lower receptor (1.00 mM) or higher Li$^+$ concentrations, the amounts were varied accordingly. No binding was observed for potassium or cesium acetate.

^{1}H NMR Data for Selected Trimeric Complexes. Complex 1−L1: ^{1}H NMR (400 MHz, D$_2$O): δ 1.40−1.85 (m, br, 18H, CH$_2$, piperidine), 2.88 (m, br, 12H, NCH$_2$, piperidine), 3.79 (d, ^2J = 13 Hz, 3H, NCH$_2$), 4.01 (d, ^2J = 13 Hz, 3H, NCH$_2$), 5.78 (s, 15H, C$_6$H$_6$), 5.82 (d, ^3J = 7 Hz, 3H, CH, pyridone), 6.77 (d, ^3J = 7 Hz, 3H, CH, pyridone).

Complex 1−L1 × Li$^+$: ^{1}H NMR (400 MHz, D$_2$O): δ 1.45−1.85 (m, br, 18H, CH$_2$, piperidine), 2.83 (m, br, 12H, NCH$_2$, piperidine), 3.91 (d, ^2J = 13 Hz, 3H, NCH$_2$), 4.03 (d, ^2J = 13 Hz, 3H, NCH$_2$), 5.90 (s, 15H, C$_6$H$_6$), 6.08 (d, ^3J = 6 Hz, 3H, CH, pyridone), 6.92 (d, ^3J = 6 Hz, 3H, CH, pyridone). ^{7}Li NMR (156 MHz, D$_2$O): δ −0.35.

Complex 2−L1: ^{1}H NMR (400 MHz, D$_2$O): δ 1.35−1.95 (m, br, 18H, CH$_2$, piperidine), 2.00 (s, 9H, C*H*$_3$C$_6$H$_5$), 2.60−3.60 (m, br, 12H, NCH$_2$, piperidine), 3.83 (d, ^2J = 13 Hz, 3H, NCH$_2$), 4.03 (d, ^2J = 13 Hz, 3H, NCH$_2$), 5.24 (d, ^3J = 6 Hz, 3H, C$_6$H$_5$Me), 5.49 (t, ^3J = 6 Hz, 3H, C$_6$H$_5$Me), 5.56 (d, ^3J = 6 Hz, 3H, C$_6$H$_5$Me), 5.83 (m, 6H, C$_6$*H*$_5$Me, pyridone), 6.08 (t, ^3J = 6 Hz, 3H, C$_6$H$_5$Me), 6.75 (d, ^3J = 6 Hz, 3H, CH, pyridone).

Complex 2−L1 × Li$^+$: ^{1}H NMR (400 MHz, D$_2$O): δ 1.35−1.95 (m, br, 18H, CH$_2$, piperidine), 1.88 (s, 9H, C*H*$_3$C$_6$H$_5$), 2.60−3.60 (m, br, 12H, NCH$_2$, piperidine), 3.97 (d, ^2J = 13 Hz, 3H, NCH$_2$), 4.10 (d, ^2J = 13 Hz, 3H, NCH$_2$), 5.26 (d, ^3J = 6 Hz, 3H, C$_6$H$_5$Me), 5.68 (m,

(39) Kang, J. W.; Maitlis, P. M. *J. Organomet. Chem.* **1971**, *30*, 127−133.
(40) Svetlanova-Larsen, A.; Zoch, C. R.; Hubbard, J. L. *Organometallics* **1996**, *15*, 3076−3087.

6H, C$_6$H$_5$Me), 6.11 (m, 6H, C$_6$H$_5$Me, pyridone), 6.23 (t, ^3J = 6 Hz, 3H, C$_6$H$_5$Me), 6.92 (d, ^3J = 6 Hz, 3H, CH, pyridone). ^{7}Li NMR (156 MHz, D$_2$O): δ −0.37.

Complex 3−L1: ^{1}H NMR (400 MHz, D$_2$O): δ 1.26 (d, ^3J = 7 Hz, 9H, CH(CH_3)$_2$), 1.28 (d, ^3J = 7 Hz, 9H, CH(CH_3)$_2$), 1.40−2.05 (m, br, 18H, CH$_2$, piperidine), 1.84 (s, 9H, CH_3C$_6$H$_4^i$Pr), 2.81 (sept, ^3J = 7 Hz, 3H, CH(CH$_3$)$_2$), 2.98 (m, br, 12H, NCH$_2$, piperidine), 3.77 (d, ^2J = 13 Hz, 3H, NCH$_2$), 4.07 (d, ^2J = 13 Hz, 3H, NCH$_2$), 5.27 (d, ^3J = 6 Hz, 3H, MeC$_6$H$_4^i$Pr), 5.52 (d, ^3J = 6 Hz, 3H, MeC$_6$H$_4^i$Pr), 5.80 (d, ^3J = 5 Hz, 3H, MeC$_6$H$_4^i$Pr), 5.81 (d, ^3J = 6 Hz, 3H, CH, pyridone), 6.04 (d, ^3J = 6 Hz, 3H, MeC$_6$H$_4^i$Pr), 6.69 (d, ^3J = 6 Hz, 3H, CH, pyridone).

Complex 3−L1 × Li$^+$: ^{1}H NMR (400 MHz, D$_2$O): δ 1.24 (d, ^3J = 7 Hz, 9H, CH(CH_3)$_2$), 1.27 (d, ^3J = 7 Hz, 9H, CH(CH_3)$_2$), 1.35−2.10 (m, br, 18H, CH$_2$, piperidine), 1.78 (s, 9H, CH_3C$_6$H$_4^i$Pr), 2.79 (sept, ^3J = 7 Hz, 3H, CH(CH$_3$)$_2$), 2.99 (m, br, 12H, NCH$_2$, piperidine), 3.90 (d, ^2J = 13 Hz, 3H, NCH$_2$), 4.12 (d, ^2J = 13 Hz, 3H, NCH$_2$), 5.29 (d, ^3J = 5 Hz, 3H, MeC$_6$H$_4^i$Pr), 5.73 (d, ^3J = 6 Hz, 3H, MeC$_6$H$_4^i$Pr), 6.03 (d, ^3J = 6 Hz, 3H, MeC$_6$H$_4^i$Pr), 6.09 (d, ^3J = 6 Hz, 3H, CH, pyridone), 6.19 (d, ^3J = 5 Hz, 3H, MeC$_6$H$_4^i$Pr), 6.86 (d, ^3J = 6 Hz, 3H, CH, pyridone). ^{7}Li NMR (156 MHz, D$_2$O): δ −0.40.

Complex 3−L2: ^{1}H NMR (400 MHz, D$_2$O): δ 1.26 (d, ^3J = 7 Hz, 9H, CH(CH_3)$_2$), 1.29 (d, ^3J = 7 Hz, 9H, CH(CH_3)$_2$), 1.83 (s, 9H, CH_3C$_6$H$_4^i$Pr), 2.81 (sept, ^3J = 7 Hz, 3H, CH(CH$_3$)$_2$), 3.03 (m, br, 12H, NCH$_2$, morpholine), 3.76 (d, ^2J = 13 Hz, 3H, NCH$_2$), 3.85 (m, br, 12H, OCH$_2$, morpholine), 4.11 (d, ^2J = 13 Hz, 3H, NCH$_2$), 5.27 (d, ^3J = 6 Hz, 3H, MeC$_6$H$_4^i$Pr), 5.51 (d, ^3J = 6 Hz, 3H, MeC$_6$H$_4^i$Pr), 5.80 (d, ^3J = 7 Hz, 3H, CH, pyridone), 5.82 (d, ^3J = 7 Hz, 3H, MeC$_6$H$_4^i$Pr), 6.05 (d, ^3J = 6 Hz, 3H, MeC$_6$H$_4^i$Pr), 6.70 (d, ^3J = 6 Hz, 3H, CH, pyridone).

Complex 3−L2 × Li$^+$: ^{1}H NMR (400 MHz, D$_2$O): δ 1.24 (d, ^3J = 7 Hz, 9H, CH(CH_3)$_2$), 1.27 (d, ^3J = 7 Hz, 9H, CH(CH_3)$_2$), 1.77 (s, 9H, CH_3C$_6$H$_4^i$Pr), 2.79 (sept, ^3J = 7 Hz, 3H, CH(CH$_3$)$_2$), 3.03 (m, br, 12H, NCH$_2$, morpholine), 3.85 (m, br, 15H, OCH$_2$, morpholine, NCH$_2$), 4.13 (d, ^2J = 15 Hz, 3H, NCH$_2$), 5.28 (d, ^3J = 7 Hz, 3H, MeC$_6$H$_4^i$Pr), 5.72 (d, ^3J = 6 Hz, 3H, MeC$_6$H$_4^i$Pr), 6.04 (d, ^3J = 6 Hz, 3H, MeC$_6$H$_4^i$Pr), 6.09 (d, ^3J = 6 Hz, 3H, CH, pyridone), 6.19 (d, ^3J = 5 Hz, 3H, MeC$_6$H$_4^i$Pr), 6.86 (d, ^3J = 6 Hz, 3H, CH, pyridone). ^{7}Li NMR (156 MHz, D$_2$O): δ −0.40.

Complex 3−L3: ^{1}H NMR (400 MHz, D$_2$O): δ 1.22 (d, ^3J = 7 Hz, 9H, CH(CH_3)$_2$), 1.28 (d, ^3J = 7 Hz, 9H, CH(CH_3)$_2$), 1.77 (s, 9H, CH$_3$, CH_3C$_6$H$_4^i$Pr), 1.85−2.95 (m, br, 24H, CH$_2$, piperazine), 2.18 (s, 9H, NCH$_3$), 2.76 (sept, ^3J = 7 Hz, 3H, CH(CH$_3$)$_2$), 3.20 (d, ^2J = 13 Hz, 3H, NCH$_2$), 3.37 (d, ^2J = 13 Hz, 3H, NCH$_2$), 5.22 (d, ^3J = 6 Hz, 3H, MeC$_6$H$_4^i$Pr), 5.41 (d, ^3J = 6 Hz, 3H, MeC$_6$H$_4^i$Pr), 5.71 (d, ^3J = 6 Hz, 3H, MeC$_6$H$_4^i$Pr), 5.74 (d, ^3J = 7 Hz, 3H, CH, pyridone), 5.98 (d, ^3J = 6 Hz, 3H, MeC$_6$H$_4^i$Pr), 6.62 (d, ^3J = 7 Hz, 3H, CH, pyridone).

Complex 3−L3 × Li$^+$: ^{1}H NMR (400 MHz, D$_2$O): δ 1.23 (d, ^3J = 7 Hz, 9H, CH(CH_3)$_2$), 1.25 (d, ^3J = 7 Hz, 9H, CH(CH_3)$_2$), 1.73 (s, 9H, CH$_3$, CH_3C$_6$H$_4^i$Pr), 1.80−2.95 (m, br, 24H, CH$_2$, piperazine), 2.21 (s, 9H, NCH$_3$), 2.75 (sept, ^3J = 7 Hz, 3H, CH(CH$_3$)$_2$), 3.29 (d, ^2J = 13 Hz, 3H, NCH$_2$), 3.45 (d, ^2J = 13 Hz, 3H, NCH$_2$), 5.23 (m, br, 3H, MeC$_6$H$_4^i$Pr), 5.66 (d, ^3J = 6 Hz, 3H, MeC$_6$H$_4^i$Pr), 5.97 (d, ^3J = 6 Hz, 3H, MeC$_6$H$_4^i$Pr), 6.00 (d, ^3J = 6 Hz, 3H, CH, pyridone), 6.13 (m, br, 3H, MeC$_6$H$_4^i$Pr), 6.77 (d, ^3J = 6 Hz, 3H, CH, pyridone). ^{7}Li NMR (156 MHz, D$_2$O): δ −0.43.

Complex 3−L4: ^{1}H NMR (400 MHz, D$_2$O): δ 1.26 (d, ^3J = 7 Hz, 9H, CH(CH_3)$_2$), 1.28 (d, ^3J = 8 Hz, 9H, CH(CH_3)$_2$), 1.82 (s, 9H, CH_3C$_6$H$_4^i$Pr), 2.69 (s, 18H, NMe$_2$), 2.82 (sept, ^3J = 7 Hz, 3H, CH(CH$_3$)$_2$), 3.86 (d, ^2J = 13 Hz, 3H, NCH$_2$), 4.18 (d, ^2J = 13 Hz, 3H, NCH$_2$), 5.26 (d, ^3J = 6 Hz, 3H, MeC$_6$H$_4^i$Pr), 5.51 (d, ^3J = 6 Hz, 3H, MeC$_6$H$_4^i$Pr), 5.79 (d, ^3J = 7 Hz, 3H, CH, pyridone), 5.81 (d, ^3J = 6 Hz, 3H, MeC$_6$H$_4^i$Pr), 6.05 (d, ^3J = 6 Hz, 3H, MeC$_6$H$_4^i$Pr), 6.72 (d, ^3J = 6 Hz, 3H, CH, pyridone).

Complex 3−L4 × Li$^+$: ^{1}H NMR (400 MHz, D$_2$O): δ 1.23 (d, ^3J = 7 Hz, 9H, CH(CH_3)$_2$), 1.27 (d, ^3J = 7 Hz, 9H, CH(CH_3)$_2$), 1.78 (s, 9H,

Table 5. Crystallographic Data for Complexes **13** and **14**

	13·0.5CH$_2$Cl$_2$	14·0.5CHCl$_3$
empirical formula	C$_{23.5}$H$_{35}$Cl$_3$N$_2$O$_2$Ru	C$_{22.5}$H$_{32.5}$Cl$_{3.5}$N$_2$O$_3$Ru
molecular weight [g mol^{-1}]	584.96	614.15
crystal size	0.22 × 0.14 × 0.09	0.18 × 0.16 × 0.09
crystal system	monoclinic	monoclinic
space group	$P2_1/n$	$P2_1/c$
a [Å]	8.7505(8)	9.3253(6)
b [Å]	21.6323(15)	16.161(5)
c [Å]	13.6254(8)	17.709(12)
α [deg]	90	90
β [deg]	95.697(6)	94.734(14)
γ [deg]	90	90
volume [Å^3]	2566.5(3)	2659.7(12)
Z	4	4
density [g cm^{-3}]	1.514	1.509
temperature [K]	140(2)	140(2)
absorption coefficient [mm^{-1}]	0.946	0.967
Θ range [deg]	3.00 to 25.03	2.85 to 25.02
index ranges	−9 → 9, −25 → 25, −16 → 16	−10 → 10, −19 → 19, −21 → 21
reflns collected	14809	16307
independent reflns	4266 (R_{int} = 0.0382)	4434 (R_{int} = 0.0439)
absorption correction	semiempirical	semiempirical
max and min transmission	0.9486 and 0.7834	0.9471 and 0.8191
data/restraints/params	4266/0/289	4434/0/308
goodness-of-fit on F^2	1.066	1.188
final R indices [$I > 2\sigma(I)$]	R1 = 0.0422, wR2 = 0.1157	R1 = 0.0527, wR2 = 0.1481
R indices (all data)	R1 = 0.0536, wR2 = 0.123	R1 = 0.0679, wR2 = 0.1659
largest diff. peak/hole [e Å^{-3}]	1.653/−1.261	0.823/−0.875

CH_3C$_6$H$_4^i$Pr), 2.70 (s, 18H, NMe$_2$), 2.79 (sept, ^3J = 7 Hz, 3H, CH(CH$_3$)$_2$), 3.97 (d, ^2J = 13 Hz, 3H, NCH$_2$), 4.14 (d, ^2J = 13 Hz, 3H, NCH$_2$), 5.29 (d, ^3J = 5 Hz, 3H, MeC$_6$H$_4^i$Pr), 5.72 (d, ^3J = 6 Hz, 3H, MeC$_6$H$_4^i$Pr), 6.05 (d, ^3J = 6 Hz, 6H, MeC$_6$H$_4^i$Pr, pyridone), 6.17 (d, ^3J = 5 Hz, 3H, MeC$_6$H$_4^i$Pr), 6.89 (d, ^3J = 6 Hz, 3H, CH, pyridone). ^{7}Li NMR (156 MHz, D$_2$O): δ −0.40.

Complex 4−L1: ^{1}H NMR (400 MHz, D$_2$O): δ 1.23 (t, ^3J = 7 Hz, 9H, CO$_2$CH$_2$CH_3), 1.35−2.05 (m, br, 18H, CH$_2$, piperidine), 2.55−3.55 (m, 12H, NCH$_2$, piperidine), 3.85 (d, ^2J = 13 Hz, 3H, NCH$_2$), 4.02 (d, ^2J = 13 Hz, 3H, NCH$_2$), 4.26 (q, ^3J = 7 Hz, 6H, CO$_2$CH_2-CH$_3$), 5.84 (d, ^3J = 7 Hz, 3H, C$_5$H$_5$CO$_2$Et), 5.98 (m, 6H, CH, C$_5$H$_5$-CO$_2$Et), 6.16 (t, ^3J = 6 Hz, 3H, CH, C$_5$H$_5$CO$_2$Et), 6.56 (m, 6H, CH, C$_5$H$_5$CO$_2$Et, pyridone), 6.77 (d, ^3J = 6 Hz, 3H, CH, pyridone).

Complex 4−L1 × Li$^+$: ^{1}H NMR (400 MHz, D$_2$O): δ 1.25 (t, ^3J = 7 Hz, 9H, CO$_2$CH$_2$CH_3), 1.35−2.05 (m, br, 18H, CH$_2$, piperidine), 2.60−3.60 (m, 12H, NCH$_2$, piperidine), 3.97 (d, ^2J = 13 Hz, 3H, NCH$_2$), 4.12 (d, ^2J = 13 Hz, 3H, NCH$_2$), 4.30 (q, ^3J = 7 Hz, 6H, CO$_2$CH_2CH$_3$), 6.10−6.30 (m, 12H, CH, C$_5$H$_5$CO$_2$Et), 6.72 (d, ^3J = 6 Hz, 3H, CH, C$_5$H$_5$CO$_2$Et or pyridone), 6.77 (d, ^3J = 6 Hz, 3H, CH, C$_5$H$_5$CO$_2$Et or pyridone), 6.87 (d, ^3J = 5 Hz, 3H, CH, pyridone). ^{7}Li NMR (156 MHz, D$_2$O): δ −0.45.

Complex 6−L1: ^{1}H NMR (400 MHz, D$_2$O): δ 1.45−1.85 (m, br, 18H, CH$_2$, piperidine), 2.95 (m, br, 12H, NCH$_2$, piperidine), 3.92 (d, ^2J = 13 Hz, 3H, NCH$_2$), 4.07 (d, ^2J = 13 Hz, 3H, NCH$_2$), 5.77 (s, 15H, Cp), 5.98 (d, ^3J = 6 Hz, 3H, CH, pyridone), 6.92 (d, ^3J = 6 Hz, 3H, CH, pyridone).

Complex 6−L1 × Li$^+$: ^{1}H NMR (400 MHz, D$_2$O): δ 1.35−1.90 (m, br, 18H, CH$_2$, piperidine), 2.92 (m, br, 12H, NCH$_2$, piperidine), 4.04 (d, ^2J = 13 Hz, 3H, NCH$_2$), 410 (d, ^2J = 13 Hz, 3H, NCH$_2$), 5.90 (s, 15H, Cp), 6.23 (d, ^3J = 6 Hz, 3H, CH, pyridone), 7.05 (d, ^3J = 6 Hz, 3H, CH, pyridone). ^{7}Li NMR (156 MHz, D$_2$O): δ −0.05.

Table 6. Crystallographic Data for Complexes **15** and **16**

	15·0.5CHCl₃	**16**·3H₂O
empirical formula	$C_{20.5}H_{30.5}Cl_{3.5}N_2O_2Ru$	$C_{60}H_{84}N_6O_{12}Ru_3$
molecular weight [g mol⁻¹]	562.11	1384.54
crystal size	0.19 × 0.15 × 0.09	0.25 × 0.19 × 0.13
crystal system	monoclinic	monoclinic
space group	$P2_1/c$	$P2_1/n$
a [Å]	8.8640(10)	13.0075(9)
b [Å]	18.626(6)	24.6431(14)
c [Å]	14.885(5)	18.6453(9)
α [deg]	90	90
β [deg]	100.814(19)	90.045(5)
γ [deg]	90	90
volume [Å³]	2413.9(12)	5976.7(6)
Z	4	4
density [g cm⁻³]	1.547	1.539
temperature [K]	140(2)	140(2)
absorption coefficient [mm⁻¹]	1.056	0.815
Θ range [deg]	2.99 to 25.02	2.71 to 25.03
index ranges	−9 → 10, −22 → 22, −15 → 17	−15 → 15, −29 → 29, −21 → 18
reflns collected	14850	34821
independent reflns	4033 (R_{int} = 0.0434)	10178 (R_{int} = 0.0433)
absorption correction	semiempirical	semiempirical
max and min transmission	0.8949 and 0.8213	0.9680 and 0.8113
data/restraints/params	4033/0/281	10178/0/740
goodness-of-fit on F^2	1.213	1.071
final R indices [$I > 2\sigma(I)$]	R1 = 0.0451, wR2 = 0.1221	R1 = 0.0479, wR2 = 0.1180
R indices (all data)	R1 = 0.0625, wR2 = 0.1339	R1 = 0.0659, wR2 = 0.1276
largest diff. peak/hole [e Å⁻³]	0.584/−0.641	1.650/−1.391

Table 7. Crystallographic Data for Complexes **17** and **18**

	17·H₂O·2C₆H₆	**18**·4.5C₆H₆
empirical formula	$C_{75}H_{101}N_9O_7Ru_3$	$C_{90}H_{117}N_9O_6Rh_3$
molecular weight [g mol⁻¹]	1543.86	1729.66
crystal size	0.16 × 0.15 × 0.15	0.26 × 0.26 × 0.26
crystal system	triclinic	cubic
space group	$P\bar{1}$	$I23$
a [Å]	15.289(3)	26.0844(7)
b [Å]	15.347(3)	26.0844(7)
c [Å]	16.3869(11)	26.0844(7)
α [deg]	103.747(11)	90
β [deg]	97.591(11)	90
γ [deg]	95.256(16)	90
volume [Å³]	3672.0(10)	17747.7(8)
Z	2	8
density [g cm⁻³]	1.396	1.295
temperature [K]	293(2)	140(2)
absorption coefficient [mm⁻¹]	0.667	0.606
Θ range [deg]	2.83 to 25.03	2.92 to 25.02
index ranges	−18 → 18, −18 → 17, −18 → 18	−29 → 29, −31 → 31, −31 → 30
reflns collected	23883	55759
independent reflns	12170 (R_{int} = 0.0343)	5230 (R_{int} = 0.0526)
absorption correction	semiempirical	none
max and min transmission	0.9480 and 0.8733	
data/restraints/params	12170/0/848	5230/0/325
goodness-of-fit on F^2	1.104	1.110
final R indices [$I > 2\sigma(I)$]	R1 = 0.0655, wR2 = 0.1783	R1 = 0.0265, wR2 = 0.0648
R indices (all data)	R1 = 0.0825, wR2 = 0.2039	R1 = 0.0290, wR2 = 0.0656
largest diff. peak/hole [e Å⁻³]	1.957/−1.086	0.362/−0.414

Complex 7−L1: ¹H NMR (400 MHz, D₂O): δ 1.35−2.00 (m, br, 18H, CH₂, piperidine), 1.45 (s, 9H, CH₃), 1.59 (s, 9H CH₃), 1.70 (s, 9H, CH₃), 1.86 (s, 9H, CH₃), 2.70−3.55 (m, br, 12H, NCH₂, piperidine), 3.86 (d, ^2J = 13 Hz, 3H, NCH₂), 4.09 (d, ^2J = 13 Hz, 3H, NCH₂), 5.29 (s, 3H, C₅Me₄*H*), 5.87 (d, ^3J = 6 Hz, 3H, CH, pyridone), 6.75 (d, ^3J = 6 Hz, 3H, CH, pyridone).

Complex 7−L1 × Li⁺: ¹H NMR (400 MHz, D₂O): δ 1.25−2.10 (m, br, 18H, CH₂, piperidine), 1.35 (s, 9H, CH₃), 1.52 (s, 9H, CH₃), 1.73 (s, 9H, CH₃), 1.88 (s, 9H, CH₃), 2.60−3.60 (m, br, 12H, NCH₂, piperidine), 4.00 (d, ^2J = 13 Hz, 3H, NCH₂), 4.15 (d, ^2J = 13 Hz, 3H, NCH₂), 5.64 (s, 3H, C₅Me₄*H*), 6.15 (d, ^3J = 6 Hz, 3H, CH, pyridone), 6.85 (d, ^3J = 6 Hz, 3H, CH, pyridone). ⁷Li NMR (156 MHz, D₂O): δ 0.08.

Complex 7−L3: ¹H NMR (400 MHz, D₂O): δ 1.47 (s, 9H, CH₃), 1.60 (s, 9H, CH₃), 1.74 (s, 9H, CH₃), 1.88 (s, 9H, CH₃), 2.05−3.10 (m, br, 24H, CH₂, piperazine), 2.24 (s, 9H, NCH₃, piperazine), 3.35 (d, ^2J = 13 Hz, 3H, NCH₂), 3.44 (d, ^2J = 13 Hz, 3H, NCH₂), 5.31 (s, 3H, C₅Me₄*H*), 5.83 (d, ^3J = 6 Hz, 3H, CH, pyridone), 6.79 (d, ^3J = 6 Hz, 3H, CH, pyridone).

Complex 7−L3 × Li⁺: ¹H NMR (400 MHz, D₂O): δ 1.32 (s, 9H, CH₃), 1.47 (s, 9H, CH₃), 1.76 (s, 9H, CH₃), 1.91 (s, 9H, CH₃), 2.05−3.05 (m, br, 24H, CH₂, piperazine), 2.21 (s, 9H, NCH₃, piperazine), 3.41 (d, ^2J = 14 Hz, 3H, NCH₂), 3.49 (d, ^2J = 14 Hz, 3H, NCH₂), 5.63 (s, 3H, C₅Me₄*H*), 6.07 (d, ^3J = 6 Hz, 3H, CH, pyridone), 6.86 (d, ^3J = 6 Hz, 3H, CH, pyridone). ⁷Li NMR (156 MHz, D₂O): δ 0.03.

Complex 8−L1: ¹H NMR (400 MHz, D₂O): δ 1.40−1.90 (m, br, 18H, CH₂, piperidine), 1.72 (s, 45H, Cp*), 2.80−3.35 (m, br, 12H, CH₂, piperidine), 3.85 (d, ^2J = 13 Hz, 3H, NCH₂), 4.00 (d, ^2J = 13 Hz, 3H, NCH₂), 5.76 (d, ^3J = 7 Hz, 3H, CH, pyridone), 6.70 (d, ^3J = 7 Hz, 3H, CH, pyridone).

Complex 8−L1 × Li⁺: ¹H NMR (400 MHz, D₂O): δ 1.35−1.95 (m, br, 18H, CH₂, piperidine), 1.70 (s, 45H, Cp*), 2.75−3.25 (m, br,

12H, CH₂, piperidine), 3.92 (d, ^2J = 14 Hz, 3H, NCH₂), 4.01 (d, ^2J = 13 Hz, 3H, NCH₂), 6.19 (d, ^3J = 6 Hz, 3H, CH, pyridone), 685 (d, ^3J = 6 Hz, 3H, CH, pyridone). ⁷Li NMR (156 MHz, D₂O): δ 0.07.

Complex 9−L1: ¹H NMR (400 MHz, D₂O): δ 1.35−2.05 (m, br, 18H, CH₂, piperidine), 1.50 (s, 9H, CH₃), 1.53 (s, 9H, CH₃), 1.65 (s, 9H, CH₃), 1.81 (s, 9H, CH₃), 2.70−3.50 (m, br, 12H, NCH₂, piperidine), 3.92 (d, ^2J = 13 Hz, 3H, NCH₂), 4.16 (d, ^2J = 13 Hz, 3H, NCH₂), 5.40 (s, 3H, Me₄C₅*H*), 5.89 (d, ^3J = 7 Hz, 3H, CH, pyridone), 6.83 (d, ^3J = 7 Hz, 3H, CH, pyridone).

Complex 9−L1 × Li⁺: ¹H NMR (400 MHz, D₂O): δ 1.35 (s, 9H, CH₃), 1.40 (s, 9H, CH₃), 1.45−1.95 (m, br, 18H, CH₂, piperidine), 1.69 (s, 9H, CH₃), 1.85 (s, 9H, CH₃), 3.03 (m, br, 12H, NCH₂, piperidine), 4.00 (d, ^2J = 13 Hz, 3H, NCH₂), 4.19 (d, ^2J = 13 Hz, 3H, NCH₂), 5.77 (s, 3H, Me₄C₅*H*), 6.18 (d, ^3J = 6 Hz, 3H, CH, pyridone), 6.91 (d, ^3J = 6 Hz, 3H, CH, pyridone). ⁷Li NMR (156 MHz, D₂O): δ −0.55.

Complex 10−L1: ¹H NMR (400 MHz, D₂O): δ 1.45−1.95 (m, br, 18H, CH₂, piperidine), 1.67 (s, 45H, Cp*), 3.04 (m, br, 12H, NCH₂, piperidine), 3.90 (d, ^2J = 13 Hz, 3H, NCH₂), 4.09 (d, ^2J = 13 Hz, 3H, NCH₂), 5.81 (d, ^3J = 7 Hz, 3H, CH, pyridone), 6.78 (d, ^3J = 7 Hz, 3H, CH, pyridone).

Complex 10−L1 × Li⁺: ¹H NMR (400 MHz, D₂O): δ 1.35−2.05 (m, br, 18H, CH₂, piperidine), 1.64 (s, 45H, Cp*), 3.03 (m, br, 12H, NCH₂, piperidine), 3.96 (d, ^2J = 13 Hz, 3H, NCH₂), 4.17 (d, ^2J = 13 Hz, 3H, NCH₂), 6.22 (d, ^3J = 6 Hz, 3H, CH, pyridone), 6.91 (d, ^3J = 6 Hz, 3H, CH, pyridone). ⁷Li NMR (156 MHz, D₂O): no data.

General Procedure for the Potentiometric Titration of Mono-meric Complexes with CsOH: A mixture of the half-sandwich complex [(π-ligand)MCl₂]₂ (75.0 μmol) and the respective ligand (150 μmol) was stirred in water (10 mL) until a clear solution was obtained. The pH was measured after adding a CsOH stock solution in steps of

Table 8. Crystallographic Data for Complex **19**

	19
empirical formula	$C_{60}H_{81}Ir_3N_6O_9$
molecular weight [g mol^{-1}]	1606.91
crystal size	$0.19 \times 0.19 \times 0.14$
crystal system	rhombohedral
space group	$R3$
a [Å]	18.832(4)
b [Å]	18.832(4)
c [Å]	13.812(5)
α [deg]	90
β [deg]	90
γ [deg]	120
volume [Å^3]	4242.3(19)
Z	3
density [g cm^{-3}]	1.887
temperature [K]	140(2)
absorption coefficient [mm^{-1}]	7.104
Θ range [deg]	2.90 to 25.02
index ranges	$-22 \rightarrow 19$, $-22 \rightarrow 22$, $-16 \rightarrow 16$
reflns collected	8956
independent reflns	3304 (R_{int} = 0.0498)
absorption correction	semiempirical
max and min transmission	0.4041 and 0.3390
Data/restraints/params	3304/1/235
goodness-of-fit on F^2	1.013
final R indices [$I > 2\sigma(I)$]	R1 = 0.0314, wR2 = 0.0537
R indices (all data)	R1 = 0.0388, wR2 = 0.0566
largest diff. peak/hole [e Å^{-3}]	3.388/−1.077

0.05 equiv (78 μL, 96 mM). The reaction mixture was allowed to equilibrate for 5 min after each addition of base. The concentration of the monomeric complex at the beginning of the titration was 15.0 mM.

Kinetic Measurements: A solution of LiCl in D_2O was added to a solution of complex **17** in D_2O in an NMR tube (final concn: [receptor] = 4.9 mM, [Li$^+$] = 9.8 mM). The mixture was shaken vigorously, and the ^{1}H NMR measurements were started immediately. The concentration of **17** and its Li$^+$ adduct was determined by integration of suited ^{1}H NMR signals. The cationic host was made in situ by dissolving complex **3** and **L1** in D_2O and by the subsequent addition of a stock solution of CsOH. The reaction was started by adding LiCl, as described above (final concn: [receptor] = 4.9 mM, [Li$^+$] = 9.8 mM).

Potentiometric Titration of Receptor 17 with HCl: Receptor **17** was prepared in situ by adding a solution of CsOH (3.12 mL, 96.0

mM) to a solution of complex **3** (75.0 μmol, 45.9 mg) and ligand **L3** (150 μmol, 31.2 mg) in water (6.88 mL). After addition of various amounts of a Li$^+$ stock solution (0.10 or 0.50 M), the reaction mixture was equilibrated for 3 h. The HCl solution (Titrisol) was added in steps of 0.05 equiv (76 μL, 0.1 M) for the titration (Figure 14) or in one portion of 4.5 equiv for the calibration curve (Figure 15). The solutions were allowed to equilibrate for 5 min (titration) or 10 min (calibration) before the pH was measured.

Colorimetric Test for Li$^+$: A stock solution of receptor **17** was prepared by adding a solution of CsOH (3.12 mL, 96.0 mM) to a solution of complex **3** (75.0 μmol, 45.9 mg) and ligand **L3** (150 μmol, 31.2 mg) in water (6.88 mL). The nine different samples shown in Figure 16 were made by mixing solutions of **17** (5.0 mM) and LiCl (10.0 mM) with water to obtain the given concentrations. The total volume of each sample amounts to 2.0 mL. After equilibration for 3 h, a solution of FeCl$_3$ in water was added (0.1 M, final Fe^{3+} concn: 1.7, 3.3, and 5.0 mM). The color changes occurred instantly.

Crystallographic Investigations: The relevant details of the crystals, data collection, and structure refinement are listed in Tables 5−8. Diffraction data were collected using Mo Kα radiation on different equipment and at different temperatures; a four-circle kappa goniometer, equipped with an Oxford Diffraction KM4 Sapphire CCD (**13**, **16**, and **18**) or a mar345 IPDS (**14**, **15**, **17**, and **19**). Data reduction was performed with CrysAlis RED 1.7.0.[41] Absorption correction was applied to all data sets, except that of complex **18**. In all cases, a semiempirical method (MULTI−SCAN)[42] has been employed. All structures were refined using the full-matrix least-squares on F^2 with all non-H atoms anisotropically defined. The hydrogen atoms were placed in calculated positions using the "riding model" with $U_{iso} = a \times U_{eq}$ (where a is 1.5 for methyl hydrogen atoms and 1.2 for others). Structure refinement and geometrical calculations were carried out on all structures with SHELXTL.[43]

Supporting Information Available: Additional figures and schemes. This material is available free of charge via the Internet at http://pubs.acs.org.

JA044874N

(41) Oxford Diffraction Ltd.: Abingdon, Oxfordshire, U.K., 2003.
(42) Blessing, R. H. *Acta Crystallogr., Sect. A* **1995**, *51*, 33−38.
(43) Sheldrick, G. M. *SHELXTL*; University of Göttingen: Göttingen, Germany, 1997; Bruker AXS, Inc.: Madison, WI, 1997.